Author contributions

NK designed the research, analysed the data and wrote the paper; AN, XW, YX, HS and SD collected specimens and patient data; HM, AH, KN and YT participated in the analysis and coordinated the research; SK led the entire project, designed the research and wrote the paper.

Conflict of interest

There are no relevant conflicts of interest to disclose.

Nozomu Kawashima
Atsushi Narita
Xinan Wang
Yinyan Xu
Hirotoshi Sakaguchi
Sayoko Doisaki
Hideki Muramatsu
Asahito Hama
Koji Nakanishi
Yoshiyuki Takahashi
Seiji Kojima
Department of Paediatrics, Nagoya University Graduate School of Medicine, Nagoya, Japan
E-mail: kojimas@med.nagoya-u.ac.jp

Keywords: *ALDH2*, haematopoietic stem cells, children, idiopathic aplastic anaemia, bone marrow failure

References

Bacigalupo, A., Hows, J., Gluckman, E., Nissen, C., Marsh, J., Van Lint, M.T., Congiu, M., De Planque, M.M., Ernst, P. & McCann, S. (1988) Bone marrow transplantation (BMT) versus immunosuppression for the treatment of severe aplastic anaemia (SAA): a report of the EBMT SAA working party. *British Journal of Haematology*, **70**, 177–182.

Camitta, B.M., Rappeport, J.M., Parkman, R. & Nathan, D.G. (1975) Selection of patients for bone marrow transplantation in severe aplastic anemia. *Blood*, **45**, 355–363.

Chen, C.H., Ferreira, J.C., Gross, E.R. & Mochly-Rosen, D. (2014) Targeting aldehyde dehydrogenase 2: new therapeutic opportunities. *Physiological Reviews*, **94**, 1–34.

Garaycoechea, J.I., Crossan, G.P., Langevin, F., Daly, M., Arends, M.J. & Patel, K.J. (2012) Genotoxic consequences of endogenous aldehydes on mouse haematopoietic stem cell function. *Nature*, **489**, 571–575.

Hira, A., Yabe, H., Yoshida, K., Okuno, Y., Shiraishi, Y., Chiba, K., Tanaka, H., Miyano, S., Nakamura, J., Kojima, S., Ogawa, S., Matsuo, K., Takata, M. & Yabe, M. (2013) Variant ALDH2 is associated with accelerated progression of bone marrow failure in Japanese Fanconi anemia patients. *Blood*, **122**, 3206–3209.

Kulagin, A., Lisukov, I., Ivanova, M., Golubovskaya, I., Kruchkova, I., Bondarenko, S., Vavilov, V., Stancheva, N., Babenko, E., Sipol, A., Pronkina, N., Kozlov, V. & Afanasyev, B. (2014) Prognostic value of paroxysmal nocturnal haemoglobinuria clone presence in aplastic anaemia patients treated with combined immunosuppression: results of two-centre prospective study. *British Journal of Haematology*, **164**, 546–554.

Liang, J., Yagasaki, H., Kamachi, Y., Hama, A., Matsumoto, K., Kato, K., Kudo, K. & Kojima, S. (2006) Mutations in telomerase catalytic protein in Japanese children with aplastic anemia. *Haematologica*, **91**, 656–658.

Matsuo, K., Wakai, K., Hirose, K., Ito, H., Saito, T. & Tajima, K. (2006) Alcohol dehydrogenase 2 His47Arg polymorphism influences drinking habit independently of aldehyde dehydrogenase 2 Glu487Lys polymorphism: analysis of 2,299 Japanese subjects. *Cancer Epidemiology Biomarkers and Prevention*, **15**, 1009–1013.

Tamakoshi, A., Hamajima, N., Kawase, H., Wakai, K., Katsuda, N., Saito, T., Ito, H., Hirose, K., Takezaki, T. & Tajima, K. (2003) Duplex polymerase chain reaction with confronting two-pair primers (PCR-CTPP) for genotyping alcohol dehydrogenase beta subunit (ADH2) and aldehyde dehydrogenase 2 (ALDH2). *Alcohol and Alcoholism*, **38**, 407–410.

Wang, Y., Yagasaki, H., Hama, A., Nishio, N., Takahashi, Y. & Kojima, S. (2007) Mutation of SBDS and SH2D1A is not associated with aplastic anemia in Japanese children. *Haematologica*, **92**, 1573.

Peripheral blood lymphocyte telomere length as a predictor of response to immunosuppressive therapy in childhood aplastic anemia

Hirotoshi Sakaguchi,[1,2]* Nobuhiro Nishio,[1]* Asahito Hama,[1] Nozomu Kawashima,[1] Xinan Wang,[1] Atsushi Narita,[1] Sayoko Doisaki,[1] Yinyan Xu,[1] Hideki Muramatsu,[1] Nao Yoshida,[2] Yoshiyuki Takahashi,[1] Kazuko Kudo,[3] Hiroshi Moritake,[4] Kazuhiro Nakamura,[5] Ryoji Kobayashi,[6] Etsuro Ito,[7] Hiromasa Yabe,[8] Shouichi Ohga,[9] Akira Ohara,[10] and Seiji Kojima;[1] on behalf of the Japan Childhood Aplastic Anemia Study Group

[1]Department of Pediatrics, Nagoya University Graduate School of Medicine; [2]Division of Hematology and Oncology, Children's Medical Center, Japanese Red Cross Nagoya 1st Hospital; [3]Division of Hematology and Oncology, Shizuoka Children's Hospital; [4]Division of Pediatrics, Department of Reproductive and Developmental Medicine, Faculty of Medicine, University of Miyazaki; [5]Department of Pediatrics, Hiroshima University Graduate School of Biomedical and Health Sciences; [6]Department of Pediatrics, Sapporo Hokuyu Hospital; [7]Department of Pediatrics, Hirosaki University Graduate School of Medicine; [8]Department of Cell Transplantation and Regenerative Medicine, Tokai University School of Medicine, Isehara; [9]Department of Perinatal and Pediatric Medicine, Graduate School of Medical Sciences, Kyushu University, Fukuoka; and [10]Department of Pediatrics, Toho University School of Medicine, Tokyo, Japan

HS and NN contributed equally to this work.

ABSTRACT

Predicting the response to immunosuppressive therapy could provide useful information to help the clinician define treatment strategies for patients with aplastic anemia. In our current study, we evaluated the relationship between telomere length of lymphocytes at diagnosis and the response to immunosuppressive therapy in 64 children with aplastic anemia, using flow fluorescence *in situ* hybridization. Median age of patients was ten years (range 1.5-16.2 years). Severity of the disease was classified as very severe in 23, severe in 21, and moderate in 20 patients. All patients were enrolled in multicenter studies using antithymocyte globulin and cyclosporine. The response rate to immunosuppressive therapy at six months was 52% (33 of 64). The probability of 5-year failure-free survival and overall survival were 56% (95% confidence interval (CI): 41-69%) and 97% (95%CI: 87-99%), respectively. Median telomere length in responders was -0.4 standard deviation (SD) (-2.7 to +3.0 SD) and -1.5 SD (-4.0 to +1.6 (SD)) in non-responders ($P<0.001$). Multivariate analysis showed that telomere length shorter than -1.0 SD (hazard ratio (HR): 22.0; 95%CI: 4.19-115; $P<0.001$), platelet count at diagnosis less than $25x10^9$/L (HR: 13.9; 95%CI: 2.00-96.1; $P=0.008$), and interval from diagnosis to immunosuppressive therapy longer than 25 days (HR: 4.81; 95%CI: 1.15-20.1; $P=0.031$) were the significant variables for poor response to immunosuppressive therapy. Conversely to what has been found in adult patients, measurement of the telomere length of lymphocytes at diagnosis is a promising assay in predicting the response to immunosuppressive therapy in children with aplastic anemia.

Introduction

Aplastic anemia (AA) is defined as bone marrow aplasia and peripheral blood pancytopenia; disease pathogenesis is thought to involve immune-mediated processes. The first choice of treatment for severe AA in children is hematopoietic stem cell transplantation from a human leukocyte antigen (HLA)-matched sibling donor.[1,2] However, 60-70% of children with severe AA have no matched sibling donor and receive immunosuppressive therapy (IST), consisting of antithymocyte globulin (ATG) and cyclosporine (CyA). According to previous studies in children, the response rate to IST at six months was 60-70%, with the probability of survival at five years being over 90%. On the other hand, relapses occur in 10-30% of patients who responded to IST and, overall, clonal evolution develops in 10-15% patients.[3-5] In adults, several pre-treatment biomarkers have been proposed as promising tests for predicting favorable response to IST, including the presence of either human leukocyte antigen (HLA)-DR15 or a minor population of paroxysmal nocturnal hemoglobinuria (PNH)-type cells.[6-9] However, we previously reported that neither test was useful to predict response to IST and that lower white blood cell count and shorter interval from diagnosis to IST were significant predictive markers of better response,[10] on the other hand, a National Institutes of Health (NIH) study showed that higher base-line absolute reticulocyte and lymphocyte counts were highly predictive of response to IST in adult patients.[11] These results suggest a difference in etiology of AA between adults and children.[10]

Dyskeratosis congenita (DC) is a rare inherited disease characterized by the classical mucocutaneous triad of abnormal skin pigmentation, nail dystrophy, and mucosal leukoplakia.[12] Patients with DC are unable to maintain the telomere complex that are protein-DNA structures at the end of eukaryotic chromosomes that prevent degradation and aberrant recombination of the chromosome ends,[13,14] and consequently have very short telomeres.[15] Shortened telomeres can cause a wide variety of clinical features consisting not only of

 doi:10.3324/haematol.2013.091165
The online version of this article has a Supplementary Appendix.
Manuscript received on May 12, 2013. Manuscript accepted on April 28, 2014.
Correspondence: kojimas@med.nagoya-u.ac.jp

mucocutaneous abnormalities, but also other symptoms, including bone marrow failure, pulmonary fibrosis, hepatic fibrosis, and predisposition to malignancy.[16] Several recent studies revealed cryptic forms of DC among patients with seemingly acquired AA who did not have apparent physical abnormalities.[17,18] Failure of AA patients to respond to IST may be explained by the presence of cryptic inherited bone marrow failure syndromes (IBMFSs).

Several investigators have demonstrated that telomere lengths of leukocytes in patients with AA vary widely, with an increased proportion of the patients having shorter telomeres than healthy individuals.[19,20] It is known that not only patients with typical DC, but also those with cryptic DC have very short telomeres.[21] Moreover, the telomere length in leukocytes is decreased in subsets of patients with other IBMFSs including Fanconi anemia,[22] Diamond-Blackfan anemia,[23] and Schwachman-Diamond syndrome.[24] Therefore, measuring telomere length of patients with AA at diagnosis may be useful in detecting patients with cryptic type of IBMFSs.

Recently, Scheinberg *et al.* reported that the telomere length of peripheral blood leukocytes was associated with risk of hematologic relapse, clonal evolution to myelodysplastic syndrome, and overall survival (OS), but not related to hematologic response to IST in patients with severe AA.[25] Because there was no study to validate their observation, we evaluated the relationship between telomere length in hematopoietic cells before IST and the response to IST in children with AA.

Methods

Patients

Peripheral blood samples at diagnosis and clinical records were obtained from 64 children who fulfilled entry criteria and enrolled in two prospective studies conducted by the Japan Childhood Aplastic Anemia Study Group.[26,27] Patients with acquired AA were eligible if selection criteria were satisfied (see *Online Supplementary Appendix* for details). Thirty-eight patients received horse ATG (Lymphoglobulin; Genzyme, Cambridge, MA, USA) at 15 mg/kg/day for five days and 26 received rabbit ATG (Thymoglobulin, Genzyme, Cambridge, MA, USA) at 3.75 mg/kg/day for five days. CyA (6 mg/kg/day, orally) was started on Day 1 and continued to at least Day 180. The dose was adjusted to achieve a whole blood trough level of 100-200 ng/mL. Standard supportive care was supplied in each institute. Response to IST was evaluated according to previously described criteria.[3] We defined patients with complete response or partial response at six months after IST as responders, and the other patients as non-responders. Relapse was defined by conversion to no response from a partial or complete response and/or the requirement for blood transfusions.

All samples and clinical records were collected after written informed consent had been obtained according to protocols approved by the Ethics Review Committee, Nagoya University Graduate School of Medicine (Research n. 732).

Measurements of telomere length and population of PNH clones

The average relative telomere length (RTL) of peripheral lymphocytes was measured by flow fluorescence *in situ* hybridization (flow-FISH), using a Telomere PNA kit (Dako Cytomation, Glostrup, Denmark).[28] Lymphocytes were derived from fresh peripheral blood in 38 cases and from frozen stored peripheral blood in 26 cases. We used delta RTL to compare patients' telomere length with that of age-matched healthy controls. Details of methods for measuring telomere length and definition of delta RTL are described in the *Online Supplementary Methods*. A minor population of paroxysmal nocturnal hemoglobinuria (PNH)-type granulocytes and red blood cells were also evaluated by flow cytometry according to a previously described method.[10]

Statistical analysis

We analyzed predictive variables associated with response to IST, failure-free survival (FFS; in which relapse, clonal evolution, second IST, HSCT, and death were censored), transplantation-free survival (TFS; in which HSCT and death were censored), and OS. Pre-treatment variables included patient's sex, age, etiology, disease severity, interval from diagnosis to IST, leukocyte count, lymphocyte count, neutrophil count, hemoglobin (Hb) level, platelet count, reticulocyte count, presence of HLA-DR15, presence of minor PNH clone, and delta RTL. Differences in these variables between responders and non-responders were assessed using the Mann-Whitney U-test and Fisher's exact probability test. Predictive factors with $P<0.10$ in the univariate analyses were set in the multivariate analysis (logistic regression modeling). $P<0.05$ was considered statistically significant. Measures of association were expressed as hazard ratios (HR) with 95% confidence intervals (CI). All tests were two-tailed with a type I error of less than 0.05 considered as statistically significant. All analyses were performed using STATA12.0 software (STATA, College Station, TX, USA).

Results

Pre-treatment patients' characteristics and clinical outcomes

A total of 64 patients with AA were included in this study. Patients' characteristics are shown in Table 1. The median age at IST was 10.0 years (range 1.5-16.2 years). Disease severity was assessed as very severe in 23 patients, severe in 21 patients, and moderate in 20 patients. Causes of AA were idiopathic in 60 patients and hepatitis in 4 patients. Median follow-up time from the time of IST was 35 months (range 6-132 months).

Overall, 33 of 64 patients (52%) responded to IST at six months after administration of ATG. Of the 33 responders, 4 children relapsed at 6, 34, 66, and 91 months after IST, respectively. The probability of 5-year cumulative incidence of relapse was 8% (95%CI: 2-28%). Nineteen transplantations were carried out for non-responders or patients with relapse. Of 64 children with AA, only one patient developed clonal evolution at 23 months after IST. During the observation period, 2 patients died; both of them had shown no response to IST, one suffered from lethal cerebral hemorrhage at six months, and the other underwent bone marrow transplantation from an HLA-matched unrelated donor at 12 months after IST and died of transplantation-related hepatic failure. The probability of 5-year FFS, TFS, and OS were 56% (95%CI: 41-69%), 63% (95%CI: 48-75%), and 97% (95%CI: 87-99%), respectively.

Telomere length of children with AA

Comparing SD calculated in 71 healthy individuals, median telomere length was -0.9SD (range -4.0 to +3.0SD) in all patients (n=64), -0.4SD (range -2.7 to +3.0SD) in

Table 1. Patients' characteristics.

Variables		Total	Responder	Non-responder	P
N		64	33	31	
Sex	M/F	38/26	22/11	16/15	NS
Age at diagnosis (range)	median	10.0 (1.5-16.2)	10.0 (1.5-16.2)	9.7 (2.6-15.1)	NS
Severity	VSAA/ SAA/MAA	23/21/20	12/10/11	11/11/9	NS
Etiology	Idiopathic/hepatitis	60/4	31/2	29/2	NS
ATG	Horse/rabbit	38/26	23/10	15/16	0.08
Interval from diagnosis to IST	median (range)	22 (1-341)	18 (1-85)	28 (4-341)	0.02
WBC at diagnosis ($x10^9$/L)	median (range)	2300 (20-8700)	2300 (20-8700)	2400 (300-5000)	NS
NEU at diagnosis ($x10^9$/L)	median (range)	300 (0-3130)	380 (0-3130)	260 (0-1140)	NS
LYM at diagnosis ($x10^9$/L)	median (range)	1900 (20-5600)	1800 (20-5600)	2000 (200-4300)	NS
Hb at diagnosis (g/dL)	median (range)	7.3 (2.7-11.4)	7.2 (2.8-11.0)	7.4 (2.7-11.4)	NS
PLT at diagnosis ($x10^9$/L)	median (range)	1.6 (0.3-5.4)	2.1 (0.4-5.2)	1.6 (0.3-5.4)	0.04
RET at diagnosis ($x10^9$/L)	median (range)	27 (0-96)	27 (3-96)	27 (0-75)	NS
PNH clone	Positive/negative	11/53	7/26	4/27	NS
HLA-DR15	Positive/negative	20/44	13/20	7/24	NS
delta RTL (SD)	median (range)	-0.9 (-4.0 - +3.0)	-0.4 (-2.8 - +3.0)	-1.5 (-4.0 - +1.6)	<0.001

ATG: antithymocyte globulin; F: female; Hb: hemoglobin; HLA: human leukocyte antigen; IST: immune suppressive therapy; LYM: lymphocyte count; M: male; MAA: moderate aplastic anemia; NEU: neutrophil count; NS: not significant; PLT: platelet count; PNH: paroxysmal nocturnal hemoglobinuria; RET: reticulocyte count; RTL: relative telomere length; SAA: severe aplastic anemia; SD: standard deviation; VSAA: very severe aplastic anemia; WBC: white blood cell count.

Table 2. Multivariate analyses for poor response to IST, failure-free survival, and transplantation-free survival.

	HR	95% CI	P
Multivariate analysis for response to IST			
Interval from diagnosis to IST >25 days	4.81	1.15-20.1	0.031
IST with rabbit ATG	0.79	0.16-3.96	0.77
PLT <25x10^9/L	13.9	2.00-96.1	0.008
RTL <-1SD	22	4.19-115	<0.001
Multivariate analysis for FFS			
IST with rabbit ATG	1.27	0.47-3.48	0.64
LYM >2.0x10^9/L	2.32	1.02-5.24	0.044
PLT <25x10^9/L	4.11	1.17-14.5	0.028
RTL <-1SD	2.01	0.83-4.89	0.12
Multivariate analysis for TFS			
IST with rabbit ATG	1.32	0.45-3.86	0.61
LYM >2.0x10^9/L	3.42	1.32-8.81	0.011
PLT <25x10^9/L	4.64	1.00-21.6	0.051
RTL <-1SD	2.84	1.01-7.97	0.048

ATG: antithymocyte globulin; CI: confidence interval; FFS: failure-free survival; HR: hazard ratio; IST: immunosuppressive therapy; LYM: lymphocyte count; PLT: platelet count; RTL: relative telomere length; SD: standard deviation; TFS: transplantation-free survival; MAA: moderate aplastic anemia; NEU: neutrophil count; NS: not significant; PLT: platelet count; PNH: paroxysmal nocturnal hemoglobinuria; RET: reticulocyte count; RTL: relative telomere length; SAA: severe aplastic anemia; SD: standard deviation; VSAA: very severe aplastic anemia; WBC: white blood cell count.

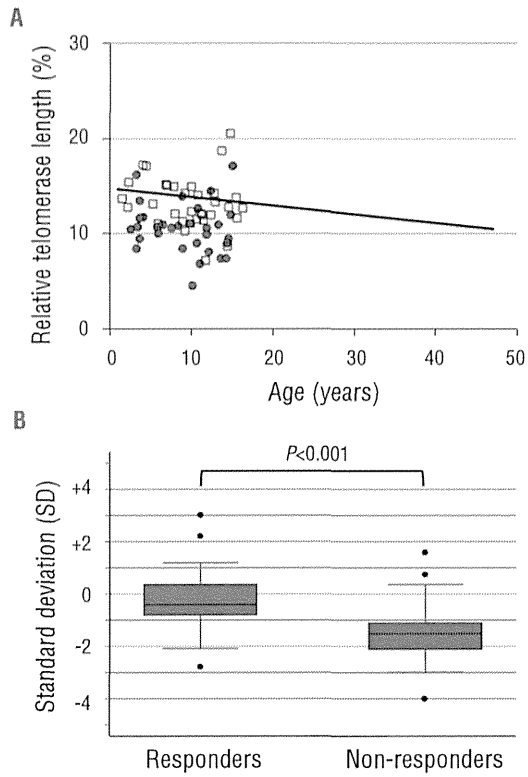

Figure 1. Relative telomere length in responders and non-responders. (A) Scatter plot of relative telomere length (RTL) *versus* age in patients with aplastic anemia (AA). The regression line for healthy individuals is shown as a solid line (Y= -0.0907X + 14.751). Results for AA patients were shown for responders (n=33; open squares) and non-responders (n=31; closed circles). (B) Comparison for telomere length between responders and non-responders. Box plots representing the distribution of telomere length in responders (n=33) and non-responders (n=31). The upper and lower limits of the boxes represent the 75th and 25th percentiles, respectively; the horizontal bar across the box indicates the median and the ends of the vertical lines indicate the minimum and maximum data values. Dots indicate outliers.

responders (n=33), and -1.5SD (range -4.0 to +1.6SD) in non-responders (n=31) (Figure 1A and B). There was a significant difference in telomere length between responders and non-responders (P<0.001). We evaluated the effects of age-adjusted telomere length quartiles on the response rate. There was a significant relationship between hematologic response and telomere length. The response rates at six months were 12.5% in the first (the shortest), 37.5% in the second, 75% in the third, and 81.3% in the fourth (the longest) quartiles of telomere length (Figure 2). The most powerful cut-off point for dividing responders and non-responders by telomere length was -1.0 SD (P=6.9x10^{-6}). There was no statistical tendency between relapse rate / clonal evolution / overall survival and telomere length.

We evaluated the pre-treatment variables for predicting response to IST in 64 children with AA (Table 1). Univariate analysis showed that interval from diagnosis to IST longer than 25 days (P=0.01), platelet count at diagnosis less than 25x10^9/L (P=0.01), and telomere length shorter than -1SD

(P<0.001) were the variables statistically significant for poor response to IST, while there were no significant differences between responders and non-responders in terms of patient age, sex, disease severity, WBC count, neutrophil count, lymphocyte count, reticulocyte count, presence of HLA-DR15, and presence of minor PNH clones. Patients with rabbit ATG showed a tendency of poorer response to IST than patients with horse ATG (P=0.08).

Multivariate analysis confirmed that telomere length shorter than -1.0SD (HR 22.0; 95%CI: 4.19-115; P<0.001), platelet count at diagnosis less than 25x10^9/L (HR 13.9; 95%CI: 2.00-96.1; P=0.008), and interval from diagnosis to IST longer than 25 days (HR 4.81; 95%CI: 1.15-20.1; P=0.031) were the significant predictive variables for poor response to IST (Table 2).

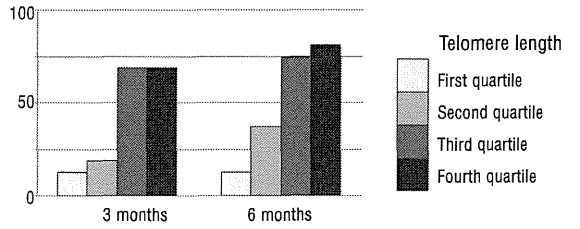

Figure 2. Response rates for immune suppressive therapy at three and six months according to telomere length. A poorer response rate was observed with each quartile as the telomere length shortened from the fourth to the first quartile.

Discussion

Our study demonstrated that the measurement of telomere length of lymphocytes is useful for predicting the response to IST in patients with AA. Recently, the NIH group reported that the telomere length of peripheral blood leukocytes was not related to hematologic response to IST, but was associated with the high risk of hematologic relapse, clonal evolution to myelodysplastic syndrome, and OS.[25] Several reasons may explain the conflicting results of the two studies. To begin with, there are several differences between the current study and the NIH study, including the methods of telomere length measurement and patients' characteristics. In the NIH study, the telomere length of pre-treatment total leukocytes was assessed by quantitative polymerase chain reaction (PCR). We measured the telomere length of lymphocytes using flow-FISH, which enabled us to measure median telomere length in the subpopulations of blood cells. Alter *et al.* compared the diagnostic sensitivity and specificity of short telomeres in different subpopulations of blood cells.[29] Their results indicated that lymphocytes were more suitable for diagnosis of DC than total leukocytes, which were a heterogeneous mixture of cell populations. The proportions of each cell population were different in each patient. The use of total leukocytes is suspected to provide less consistent results than analyses of defined leukocyte subpopulations.

Another difference between the two studies was the distribution of patients' age. Patients in our study were much younger (mean age 10 years) than those in the NIH study (mean age 35 years). Because telomeres shorten with age,[30] the differences in telomere length between patients and healthy individuals may become smaller in adults than in children. Moreover, in the NIH study, the cohort was restricted to patients with severe AA, and patients with moderate AA were not included. In contrast, 20 of 64 AA patients in our study had moderate disease. We could not estimate the frequency of clonal evolution since in our cohort there was only one patient who evolved into myelodysplastic syndrome during the observation period.

The causes of the difference in telomere length between responders and non-responders remain unknown. The short telomere length in non-responders may be ascribed to the presence of cryptic forms of IBMFS in the study cohort. Alter *et al.* reported that nearly all of the patients with both typical and cryptic DC have very short telomeres, as low as the first percentile of normal controls.[25] In our previous study, the RTLs of lymphocytes were below the 5% of normal controls in all of 6 DC patients and 2 AA patients harboring TERT mutation.[31] In the current study, there were 10 AA patients with shorter telomere length than the -2.0 SD of the cohort of healthy controls, but none of them showed clinical features of DC or had any mutation in *DKC1, TERC, TERT, NOP10, TINF2,* and *TCAB1*. It is unlikely that short telomeres in non-responders are to be ascribed to the presence of a cryptic form of DC.

Another possibility is that short telomere length may be a surrogate marker for longer disease duration that damages the hematopoietic stem cells and causes a higher number of compensatory stem cell divisions. We recently reported a significant inverse correlation between response rate to IST and interval between diagnosis and treatment in a large cohort of 312 children with newly diagnosed AA.[32] It is often difficult to determine the exact date of onset of the disease in patients with AA, especially in patients with moderate AA. The shorter telomere length may simply reflect longer duration of the disease in non-responders.

However, our study has several limitations, including a heterogeneous study population, a relatively small number of patients and a short follow-up period. To validate the results, we are conducting a prospective study to determine the optimal use of rabbit ATG for severe AA, in which we evaluate the relationship between telomere length of lymphocytes at diagnosis and the response to IST.

In conclusion, measurement of the telomere length in lymphocytes by flow-FISH is a promising assay, not only for identifying cryptic DC, but also for predicting the response to IST of patients with AA.

Acknowledgments

The authors would like to thank all contributors associated with the Japan Childhood Aplastic Anemia Study Group.

Funding

The authors supported by a grant from the Research Commitee for the dyskeratosis congenita, Ministry of Halth, and Walfare of Japan (H23-Nanchi-Japan-099) and a grant from Sanofi K.K..

Authorship and Disclosures

Information on authorship, contributions, and financial & other disclosures was provided by the authors and is available with the online version of this article at www.haematologica.org

References

1. Kojima S, Horibe K, Inaba J, Yoshimi A, Takahashi Y, Kudo K, et al. Long-term outcome of acquired aplastic anaemia in children: comparison between immunosuppressive therapy and bone marrow transplantation. Br J Haematol. 2000;111(1):321- 8.
2. Young NS. Acquired aplastic anemia. JAMA. 1999;282(3):271-8.
3. Kojima S, Hibi S, Kosaka Y, Yamamoto M, Tsuchida M, Mugishima H, et al. Immunosuppressive therapy using antithymocyte globulin, cyclosporine, and danazol with or without human granulocyte colony-stimulating factor in children with acquired aplastic anemia. Blood. 2000;96(6):2049-54.
4. Fuhrer M, Rampf U, Baumann I, Faldum A, Niemeyer C, Janka-Schaub G, et al. Immunosuppressive therapy for aplastic anemia in children: a more severe disease predicts better survival. Blood. 2005;106 (6):2102-4.
5. Locasciulli A, Oneto R, Bacigalupo A, Socie G, Korthof E, Bekassy A, et al. Outcome of patients with acquired aplastic anemia given first line bone marrow transplantation or immunosuppressive treatment in the last decade: a report from the European Group for Blood and Marrow Transplantation (EBMT). Haematologica. 2007;92(1):11-8.
6. Nakao S, Takamatsu H, Chuhjo T, Ueda M, Shiobara S, Matsuda T, et al. Identification of a specific HLA class II haplotype strongly associated with susceptibility to cyclosporine-dependent aplastic anemia. Blood. 1994;84(12):4257-61.
7. Maciejewski JP, Follmann D, Nakamura R, Saunthararajah Y, Rivera CE, Simonis T, et al. Increased frequency of HLA-DR2 in patients with paroxysmal nocturnal hemoglobinuria and the PNH/aplastic anemia syndrome. Blood. 2001;98(13):3513-9.
8. Oguz FS, Yalman N, Diler AS, Oguz R, Anak S, Dorak MT. HLA-DRB1*15 and pediatric aplastic anemia. Haematologica. 2002;87(7): 772-4.
9. Sugimori C, Chuhjo T, Feng X, Yamazaki H, Takami A, Teramura M, et al. Minor population of CD55-CD59- blood cells predicts response to immunosuppressive therapy and prognosis in patients with aplastic anemia. Blood 2006;107:1308-14.
10. Yoshida N, Yagasaki H, Takahashi Y, Yamamoto T, Liang J, Wang Y, et al. Clinical impact of HLA-DR15, a minor population of paroxysmal nocturnal haemoglobinuria-type cells, and an aplastic anaemia-associated autoantibody in children with acquired aplastic anaemia. Br J Haematol. 2008;142 (3):427-35.
11. Scheinberg P, Wu CO, Nunez O, Young NS. Predicting response to immunosuppressive therapy and survival in severe aplastic anaemia. Br J Haematol. 2009;144(2):206-16.
12. Walne AJ, Dokal I. Advances in the understanding of dyskeratosis congenita. Br J Haematol. 2009;145:164-72.
13. Greider CW, Blackburn EH. Identification of a specific telomere terminal transferase activity in Tetrahymena extracts. Cell. 1985;43(2 Pt 1):405-13.
14. Szostak JW, Blackburn EH. Cloning yeast telomeres on linear plasmid vectors. Cell. 1982;29(1):245-55.
15. Mitchell JR, Wood E, Collins K. A telomerase component is defective in the human disease dyskeratosis congenita. Nature. 1999;402:551-5.
16. Calado RT, Young NS. Telomere diseases. N Engl J Med. 2009;361:2353-65.
17. Yamaguchi H, Calado RT, Ly H, Kajigaya S, Baerlocher GM, Chanock SJ, et al. Mutations in TERT, the gene for telomerase reverse transcriptase, in aplastic anemia. N Engl J Med. 2005;352(14):1413-24.
18. Vulliamy TJ, Marrone A, Knight SW, Walne A, Mason PJ, Dokal I. Mutations in dyskeratosis congenita: their impact on telomere length and the diversity of clinical presentation. Blood. 2006;107:2680-5.
19. Ball SE, Gibson FM, Rizzo S, Tooze JA, Marsh JC, Gordon-Smith EC. Progressive telomere shortening in aplastic anemia. Blood. 1998;91(10):3582-92.
20. Brummendorf TH, Maciejewski JP, Mak J, Young NS, Lansdorp PM. Telomere length in leukocyte subpopulations of patients with aplastic anemia. Blood. 2001;97(4):895-900.
21. Yamaguchi H, Baerlocher GM, Lansdorp PM, Chanock SJ, Nunez O, Sloand E, Young NS. Mutations of the human telomerase RNA gene (TERC) in aplastic anemia and myelodysplastic syndrome. Blood. 2003;102 (3):916-8.
22. Leteurtre F, Li X, Guardiola P, Le Roux G, Sergère JC, Richard P, et al. Accelerated telomere shortening and telomerase activation in Fanconi's anaemia. Br J Haematol. 1999;105(4):883-93.
23. Pavesi E, Avondo F, Aspesi A, Quarello P, Rocci A, Vimercati C, et al. Analysis of telomeres in peripheral blood cells from patients with bone marrow failure. Pediatr Blood Cancer. 2009;53(3):411-6.
24. Thornley I, Dror Y, Sung L, Wynn RF, Freedman MH. Abnormal telomere shortening in leucocytes of children with Shwachman-Diamond syndrome. Br J Haematol. 2002;117(1):189-92.
25. Scheinberg P, Cooper JN, Sloand EM, Wu CO, Calado RT, Young NS. Association of Telomere Length of Peripheral Blood Leukocytes With Hematopoietic Relapse, Malignant Transformation, and Survival in Severe Aplastic Anemia. JAMA. 2010;304 (12):1358-64.
26. Kosaka Y, Yagasaki H, Sano K, Kobayashi R, Ayukawa H, Kaneko T, et al. Prospective multicenter trial comparing repeated immunosuppressive therapy with stem-cell transplantation from an alternative donor as second-line treatment for children with severe and very severe aplastic anemia. Blood. 2008;111:1054-9.
27. Takahashi Y, Muramatsu H, Sakata N, Hyakuna N, Hamamoto K, Kobayashi R, et al. Rabbit antithymocyte globulin and cyclosporine as first-line therapy for children with acquired aplastic anemia. Blood. 2013;121:862-3.
28. Baerlocher GM, Vulto I, de Jong G, Lansdorp PM. Flow cytometry and FISH to measure the average length of telomeres (flow FISH). Nat Protoc. 2006;1(5):2365-76.
29. Alter BP, Baerlocher GM, Savage SA, Chanock SJ, Weksler BB, Willner JP, et al. Very short telomere length by flow fluorescence in situ hybridization identifies patients with dyskeratosis congenita. Blood. 2007;110(5):1439-47.
30. Harley CB, Futcher AB, Greider CW. Telomeres shorten during ageing of human fibroblasts. Nature. 1990;345(6274):458-60.
31. Nishio N, Kojima S. Recent progress in dyskeratosis congenita. Int J Hematol. 2010;92(3):419-24.
32. Yoshida N, Yagasaki H, Hama A, Takahashi Y, Kosaka Y, Kobayashi R, et al. Predicting response to immunosuppressive therapy in childhood aplastic anemia. Haematologica. 2011;96(5):771-4.

Molecular and Virological Evidence of Viral Activation From Chromosomally Integrated Human Herpesvirus 6A in a Patient With X-Linked Severe Combined Immunodeficiency

Akifumi Endo,[1,2] Ken Watanabe,[3] Tamae Ohye,[4] Kyoko Suzuki,[5] Tomoyo Matsubara,[5] Norio Shimizu,[3] Hiroki Kurahashi,[4] Tetsushi Yoshikawa,[6] Harutaka Katano,[7] Naoki Inoue,[8] Kohsuke Imai,[1] Masatoshi Takagi,[1] Tomohiro Morio,[1] and Shuki Mizutani[1]

[1]Department of Pediatrics and Developmental Biology, Tokyo Medical and Dental University, [2]Department of Pediatrics, Tokyo Metropolitan Cancer and Infectious Diseases Center, Komagome Hospital, and [3]Department of Virology, Tokyo Medical and Dental University, [4]Division of Molecular Genetics, Fujita Health University, Toyoake; [5]Department of Pediatrics, Juntendo University Urayasu Hospital, [6]Department of Pediatrics, Fujita Health University, Toyoake, Departments of [7]Pathology and [8]Virology I, National Institute of Infectious Diseases, Tokyo, Japan

(See the Editorial Commentary by Flamand on pages 549–51.)

It has been unclear whether chromosomally integrated human herpesvirus 6 (ciHHV-6) can be activated with pathogenic effects on the human body. We present molecular and virological evidence of ciHHV-6A activation in a patient with X-linked severe combined immunodeficiency. These findings have significant implications for the management of patients with ciHHV-6.

Keywords. ciHHV-6; HHV-6; X-SCID; hemophagocytic syndrome; thrombotic microangiopathy.

Human herpesvirus 6 (HHV-6) is a ubiquitous DNA virus that is the causative agent of roseola infantum, and infects individuals by 3 years of age [1]. After primary infection, HHV-6 establishes a latent state in the host. There are 2 distinct species, HHV-6A and HHV-6B. Most HHV-6 infections are caused by HHV-6B, whereas HHV-6A is less common. Chromosomally integrated HHV-6 (ciHHV-6) is the state in which HHV-6 (HHV-6A or HHV-6B) is integrated into the host germline genome, and it is transmitted vertically in a Mendelian manner. Although ciHHV-6 affects about 1% of the general population, it is generally considered to be a nonpathogenic condition. However, it is unclear whether ciHHV-6 can be activated with pathogenic effects on the human body [2].

Severe combined immunodeficiency (SCID) is a group of genetic disorders that result in a combined absence of T- and B-cell immunity. It is characterized by life-threatening infections during the first year of life unless treated, usually with hematopoietic stem cell transplantation (HSCT). X-linked severe combined immunodeficiency (X-SCID) arises from a mutation in the interleukin 2 receptor, gamma (*IL2RG*) gene on the X-chromosome [3]. We encountered a boy with X-SCID in whom ciHHV-6A was activated.

CASE REPORT

A 2-month-old boy was hospitalized for recurrent episodes of fever, cough, diarrhea, and failure to thrive. Upon admission, a viral infection was suspected, and supportive care did not improve his symptoms.

Twenty days after admission, mild pancytopenia (leukocyte count, 1.4×10^9/L; hemoglobin level, 78 g/L; and platelet count, 37×10^9/L) and elevated aminotransferases and ferritin were evident (aspartate aminotransferase, 448 U/L; alanine aminotransferase, 218 U/L; and ferritin, 4325 ng/mL) (Supplementary Figure 1). A bone marrow biopsy showed a hypocellular condition without dysplastic changes, as well as increased activated phagocytes. These results suggested hemophagocytic syndrome (HPS).

An immunological evaluation revealed an absence of T cells and low immunoglobulin levels. Genetic analysis identified a mutation in the *IL2RG* that was consistent with X-SCID. The patient's mother was heterozygous for the same mutation, and there was no such mutation detected in the patient's father.

A comprehensive search for a pathogen identified high levels of HHV-6 DNA (1.2×10^7 copies/μg DNA) in his peripheral blood. Antiviral treatment with ganciclovir or foscarnet did not reduce the viral load, and ciHHV-6 was suspected. We detected high levels of HHV-6 DNA in the patient's fingernails, the father's peripheral blood, and the father's hair follicles (5.9×10^5, 1.0×10^7, 1.2×10^6 copies/μgDNA, respectively).

Received 7 January 2014; accepted 9 April 2014; electronically published 6 May 2014.

Correspondence: Shuki Mizutani, MD, Department of Pediatrics and Developmental Biology, Tokyo Medical and Dental University, 1-5-45, Yushima, Bunkyo-ku, Tokyo 113-8510, Japan (skkmiz@gmail.com).

Clinical Infectious Diseases 2014;59(4):545–8

DOI: 10.1093/cid/ciu323

Fluorescence in situ hybridization analysis of the patient's fibroblasts and his father's peripheral blood mononuclear cells (PBMCs) confirmed HHV-6 integration at chromosome 22 in both individuals (Figure 1); these results suggested vertical germline transmission.

However, discontinuation of antiviral treatment led to a deterioration of the patient's HPS. Because no other pathogen was detected, activation of HHV-6 was suspected. To confirm this suspicion, we performed 3 assays that could detect viral activation despite the presence of integrated HHV-6 DNA. First, reverse transcription polymerase chain reaction (RT-PCR) was used to detect viral RNA in whole-blood samples. RT-PCR was performed on 2 HHV-6 genes, the late gene U60/66 and the immediate-early (IE) gene IE1, as described previously [5]. We detected viral RNA for both genes (4.6×10^2 copies/μg RNA for U60/66 and 5.2×10^3 copies/μg RNA for IE1). Second, immunostaining was used to detect IE antigens in a bone marrow sample taken at the time of HPS (Figure 2 and Supplementary Figure 2) [6]. Last, HHV-6A was isolated from the patient's PBMCs. It was cultured with cord blood cells and its presence confirmed by immunofluorescent staining with an anti–HHV-6 monoclonal antibody (Figure 3 and Supplementary Figure 3) [1].

Two hypotheses were postulated: Either the patient with ciHHV-6 was infected de novo with HHV-6, or HHV-6 was activated from the ciHHV-6 genome present in this patient. We performed a sequence analysis of the HHV-6 IE1 gene, as IE1 is variable and readily used to distinguish between HHV-6 variants [7]. DNA samples from isolated HHV-6A (described above), the patient's fingernails, his father's hair follicles, and laboratory strains U1102 and Z29 were amplified by PCR and sequenced. Because active HHV-6 is not present in the fingernails or hair follicles, we could amplify the original integrated HHV-6 strain from the genomes in these tissues. To our surprise, the sequences and subsequent phylogenetic analysis revealed that the isolated virus was identical to the original integrated HHV-6A strain present in both the patient and his father. Furthermore, this HHV-6A strain was unique in that it differed from all other HHV-6 strains analyzed (Supplementary Figure 4). These results suggested that the isolated HHV-6A strain originated from the activation of ciHHV-6A. Analysis of 3 other viral genes (gB, U94, and DR) confirmed these results [8, 9].

The resumption of antiviral drug treatment with prednisolone ameliorated the patient's HPS. When he reached age 7 months, the patient underwent HSCT. Antiviral drug treatment was continued during HSCT, and engraftment was achieved 14 days after transplant. After engraftment, thrombotic microangiopathy (TMA) and gastrointestinal bleeding developed. Simultaneously, the patient's HHV-6A DNA and RNA titers increased, and HHV-6A was reisolated. Anticoagulant therapy and a reduction in tacrolimus dosage gradually improved the patient's TMA. With immunological reconstruction, the patient's HHV-6A DNA and RNA titers were successfully reduced and ultimately, no HHV-6A was isolated from subsequent blood samples. The asymptomatic patient was discharged at 12 months.

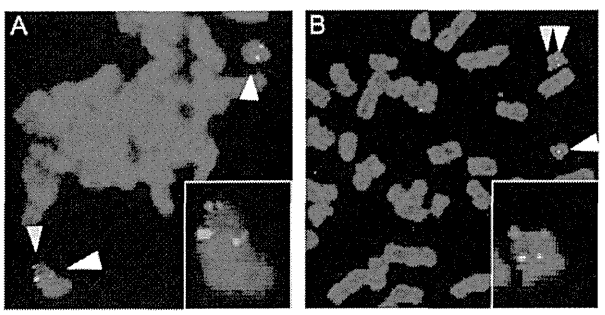

Figure 1. Integration of human herpesvirus type 6 (HHV-6) in chromosome 22 was demonstrated by fluorescence in situ hybridization analysis. Fibroblasts derived from the patient's skin (*A*) and peripheral blood mononuclear cells from the father (*B*) were cohybridized with HHV-6-specific (yellow arrow) and chromosome-22-specific probes (white arrows) [4]. HHV-6 integration in only one of the chromosome 22 alleles was shown in both materials. In sets of *A* and *B* are the enlared images of FISH data positively cohybridized with both probes.

DISCUSSION

Since the discovery of ciHHV-6 in 1993, the question of whether ciHHV-6 can be activated from its integrated state has been perpetually debated [2]. With this case report, we provide the first molecular and virological evidence of viral activation from ciHHV-6A in the human body. This evidence comprises (1) viral RNA and antigens detected in PBMCs and bone marrow, as well as HHV-6A isolated from PBMCs; (2) HHV-6A sequences integrated into the patient's and his father's genomes, which were identical to those of the isolated virus; and (3) antiviral treatment and immunological reconstruction, which were effective in treating this activated ciHHV-6A.

In an effort to understand the biological significance of ciHHV-6, active viral replication from ciHHV-6 has recently been demonstrated in vitro under specific experimental conditions [9–11]. However, only a few studies have suggested ciHHV-6 activation in vivo despite high ciHHV-6 prevalence (approximately 1%) in the general population [12–14]. Activation of ciHHV-6 in vivo has been previously reported in mothers with ciHHV-6 who passed on the infection to infants who did not have inherited ciHHV-6 [8]. Our findings are consistent with these findings, as we clearly demonstrate the activation of HHV-6A in a patient who acquired ciHHV-6 via germline transmission.

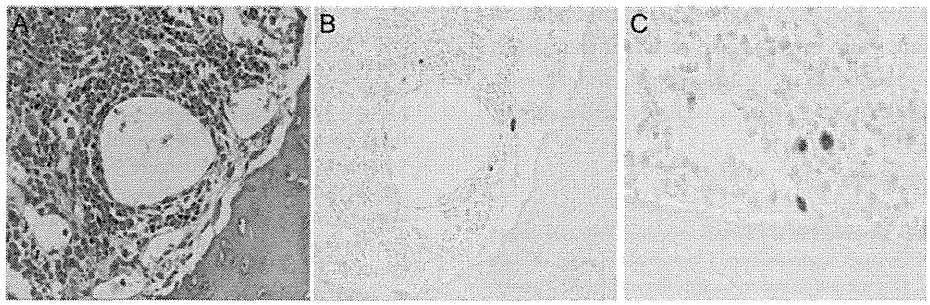

Figure 2. Histology and human herpesvirus type 6 (HHV-6) immunostaining. *A*, Hematoxylin and eosin staining of bone marrow. *B* and *C*, Immunostaining with an anti–HHV-6 antibody.

We speculate that the presence of X-SCID allowed for efficient activation of ciHHV-6A, and this phenomenon was detected with several technical strategies. Similarly, RT-PCR and virus isolation showed conversion from an HHV-6–positive status to a negative status with the patient's immunological recovery. In addition, these techniques were used to test samples taken from the patient's father. We were able to determine that he was indeed the ciHHV-6 carrier, yet he was HHV-6A negative. This suggests that X-SCID influenced the activation of ciHHV-6A. Because X-SCID prevalence is extremely low (about 0.001%), this case provides valuable insight into immunocompromised individuals and HHV-6 infection. However, the mechanism that triggered ciHHV-6A activation and replication in this patient remains to be elucidated. Further studies of patients with ciHHV-6 are required to determine what causes activation of this latent integrated virus.

The association between HHV-6 and HPS has previously been reported [15], and a link between HHV-6 and TMA has also been noted [16]. Therefore, it is possible that ciHHV-6A activation in our patient was associated with HPS and TMA. We noted that active HHV-6A infection coincided with symptom onset and the active infection was controlled with antiviral treatment. This suggests that HHV-6A is pathogenic, yet it remains to be established whether activated HHV-6A enhances underlying pathological conditions, and whether the activation of ciHHV-6A occurs in a similar fashion for all infected individuals.

Latent HHV-6 reactivation occurs in 40%–50% of recipients during HSCT, and our case report is the first to demonstrate that ciHHV-6A activation also occurs during this procedure. It is possible that the presence of X-SCID allowed for viral activation, but further studies are required to validate this hypothesis.

We have described the first case to provide molecular and virological evidence of the activation of chromosomally integrated HHV-6A in the human body. However, our report has limitations. We still do not know how virus production was triggered from a state of ciHHV-6A or how the production of the virus affected the patient's symptoms. Despite these limitations, based on this case, we hypothesize that an immunodeficient phenotype in conjunction with uncontrolled host defense systems allows the activation of ciHHV-6A. We support the recommendation that a screening program to detect ciHHV-6 in

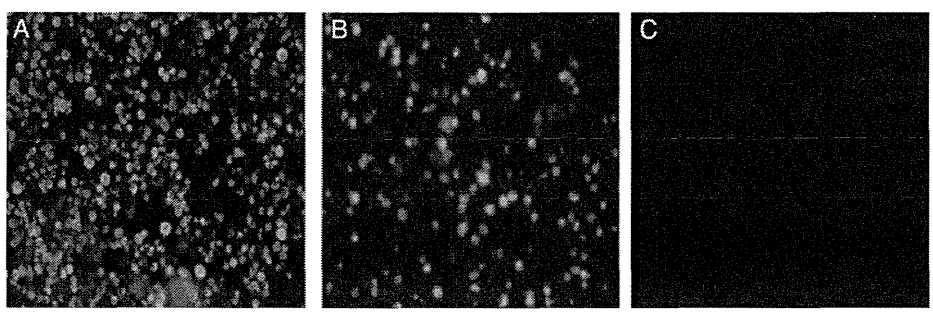

Figure 3. Immunofluorescent staining assay. *A*, Virus isolation confirmed with an anti– human herpesvirus type 6 antibody (gp116/64/54). *B*, U1102 cultured with cord blood cells (positive control). *C*, Cord blood cells alone (negative control).

transplant patients and donors be established, and recommend that ciHHV-6 patients with immunocompromised status such as primary immunodeficiency, human immunodeficiency virus infection, or organ transplantation, be monitored carefully.

Supplementary Data

Supplementary materials are available at *Clinical Infectious Diseases* online (http://cid.oxfordjournals.org). Supplementary materials consist of data provided by the author that are published to benefit the reader. The posted materials are not copyedited. The contents of all supplementary data are the sole responsibility of the authors. Questions or messages regarding errors should be addressed to the author.

Notes

Financial support. This work was supported by the Ministry of Health, Labour, and Welfare of Japan (H25 Shinko-Ippan-015 to H. Ka., H23 Nanchi-Ippan-003 and H25 Nanchitou-Menneki-Ippan-105 to T. Mo.); the Japan Society for the Promotion of Science (22590426 to N. I.); and the Ministry of Education, Culture, Sciences, and Technology in Japan (23390270 and 23390271 to T. Mo. and S. M.).

Potential conflicts of interest. All authors: No reported conflicts.

All authors have submitted the ICMJE Form for Disclosure of Potential Conflicts of Interest. Conflicts that the editors consider relevant to the content of the manuscript have been disclosed.

References

1. Yamanishi K, Shiraki K, Kondo T, et al. Identification of human herpesvirus-6 as a causal agent for exanthema subitum. Lancet **1988**; 1: 1065–7.
2. Pellett PE, Ablashi DV, Ambros PF, et al. Chromosomally integrated human herpesvirus 6: questions and answers. Rev Med Virol **2012**; 22: 144–55.
3. Sugamura K, Asao H, Kondo M, et al. The interleukin-2 receptor gamma chain: its role in the multiple cytokine receptor complexes and T cell development in XSCID. Annu Rev Immunol **1996**; 14: 179–205.
4. Isegawa Y, Mukai T, Nakano K, et al. Comparison of the complete DNA sequences of human herpesvirus 6 variants A and B. J Virol **1999**; 73: 8053–63.
5. Van den Bosch G, Locatelli G, Geerts L, et al. Development of reverse transcriptase PCR assays for detection of active human herpesvirus 6 infection. J Clin Microbiol **2001**; 39:2308–10.
6. Papanikolaou E, Kouvatsis V, Dimitriadis G, Inoue N, Arsenakis M. Identification and characterization of the gene products of open reading frame U86/87 of human herpesvirus 6. Virus Res **2002**; 89:89–101.
7. Yamamoto T, Mukai T, Kondo K, Yamanishi K. Variation of DNA sequence in immediate-early gene of human herpesvirus 6 and variant identification by PCR. J Clin Microbiol **1994**; 32:473–6.
8. Gravel A, Hall CB, Flamand L. Sequence analysis of transplacentally acquired human herpesvirus 6 DNA is consistent with transmission of a chromosomally integrated reactivated virus. J Infect Dis **2013**; 207:1585–9.
9. Arbuckle JH, Medveczky MM, Luka J, et al. The latent human herpesvirus-6A genome specifically integrates in telomeres of human chromosomes in vivo and in vitro. Proc Natl Acad Sci U S A **2010**; 107:5563–8.
10. Prusty BK, Krohne G, Rudel T. Reactivation of chromosomally integrated human herpesvirus-6 by telomeric circle formation. PLoS Genet **2013**; 9:e1004033.
11. Huang Y, Hidalgo-Bravo A, Zhang E, et al. Human telomeres that carry an integrated copy of human herpesvirus 6 are often short and unstable, facilitating release of the viral genome from the chromosome. Nucleic Acids Res **2014**; 42:315–27.
12. Kobayashi D, Kogawa K, Imai K, et al. Quantitation of human herpesvirus-6 (HHV-6) DNA in a cord blood transplant recipient with chromosomal integration of HHV-6. Transpl Infect Dis **2011**; 13:650–3.
13. Troy SB, Blackburn BG, Yeom K, Caulfield AK, Bhangoo MS, Montoya JG. Severe encephalomyelitis in an immunocompetent adult with chromosomally integrated human herpesvirus 6 and clinical response to treatment with foscarnet plus ganciclovir. Clin Infect Dis **2008**; 47: e93–6.
14. Wittekindt B, Berger A, Porto L, et al. Human herpes virus-6 DNA in cerebrospinal fluid of children undergoing therapy for acute leukaemia. Br J Haematol **2009**; 145:542–5.
15. Tanaka H, Nishimura T, Hakui M, Sugimoto H, Tanaka-Taya K, Yamanishi K. Human herpesvirus-6-associated hemophagocytic syndrome in a healthy adult. Emerg Infect Dis **2002**; 8:87–8.
16. Matsuda Y, Hara J, Miyoshi H, et al. Thrombotic microangiopathy associated with reactivation of human herpesvirus-6 following high-dose chemotherapy with autologous bone marrow transplantation in young children thrombotic microangioapathy. Bone Marrow Transplant **1999**; 24:919–23.

PEDIATRICS INTERNATIONAL Official Journal of the Japan Pediatric Society

Pediatrics International (2014) **56**, 510–514 doi: 10.1111/ped.12325

Original Article

Pneumothorax in patients with severe combined immunodeficiency

Akihiro Hoshino,[1] Kohsuke Imai,[2] Yusei Ohshima,[5] Motoko Yasutomi,[5] Masashi Kasai,[6] Masaru Terai,[7] Keiko Ishigaki,[4] Tomohiro Morio,[3] Toshio Miyawaki[1] and Hirokazu Kanegane[1]

[1]*Department of Pediatrics, Graduate School of Medicine and Pharmaceutical Sciences, University of Toyama, Toyama,* [2]*Department of Community Pediatrics, Perinatal and Maternal Medicine and* [3]*Department of Pediatrics and Developmental Biology, Graduate School of Medicine, Tokyo Medical and Dental University,* [4]*Department of Pediatrics, Tokyo Women's Medical University, School of Medicine, Tokyo,* [5]*Department of Pediatrics, Faculty of Medical Sciences, University of Fukui, Eiheiji,* [6]*Department of General Pediatrics, Nagano Children's Hospital, Azumino and* [7]*Department of Pediatrics, Tokyo Women's Medical University, Yachiyo Medical Center, Yachiyo, Japan*

Abstract ***Background***: Most infants with pneumothorax have underlying conditions. *Pneumocystis jirovecii* pneumonia (PCP) frequently occurs in patients with severe combined immunodeficiency (SCID). The aim of this study was to determine clinical features of PCP-associated pneumothorax in SCID patients.

Methods: The medical records of four SCID patients with pneumothorax were retrospectively reviewed.

Results: All four patients were diagnosed as having SCID at the time of contracting PCP. All patients received mechanical ventilation because of severe respiratory failure. Only one patient was successfully extubated and was alive following hematopoietic stem cell transplantation (HSCT); of the remaining patients, however, two died of respiratory failure, and one patient died of early HSCT-related complications.

Conclusions: Pneumothorax associated with PCP can occur in SCID patients, and they may have a poor prognosis. If pneumothorax occurs in infants, both respiratory management and prompt investigation of the underlying conditions are needed, considering the possibility of PCP associated with SCID.

Key words *Pneumocystis jirovecii*, pneumothorax, severe combined immunodeficiency.

Pneumothorax in pediatric patients occurs with the highest frequency in newborns or older adolescents, and it usually occurs without any underlying lung abnormalities.[1] Pneumothorax is notably uncommon in infants, and the investigation of the underlying conditions is important.[2] Six infants were reported to have pneumothorax,[2] including three cases of respiratory infection, two cases of anatomical abnormality, and one case of febrile seizure. Of the three patients with respiratory infection, two patients had *Pneumocystis jirovecii* infection.

Pneumocystis jirovecii pneumonia (PCP) is an important underlying condition. PCP frequently occurs in individuals with a cellular immunodeficiency, which is potentially life-threatening by itself.[3] Two patients with PCP in a previous report were diagnosed as having acquired immunodeficiency syndrome.[2]

Severe combined immunodeficiency (SCID) is a primary immunodeficiency characterized by defects in T-cell development, which results in cellular and humoral immunodeficiency.[4] Without treatment, infection can be fatal, usually within the first year of life, and hematopoietic stem cell transplantation (HSCT) or gene therapy is a life-saving treatment.[5] SCID patients are highly susceptible to a variety of bacterial, viral and opportunistic infections. Prior studies have reported that 20–73% of patients with SCID also had PCP at diagnosis.[6–8] To our knowledge, however, PCP-associated pneumothorax in SCID patients has not been reported. The aim of this study was to identify the clinical features of PCP-associated pneumothorax in SCID patients.

Correspondence: Akihiro Hoshino, MD, Department of Pediatrics, Graduate School of Medicine and Pharmaceutical Sciences, University of Toyama, 2630 Sugitani, Toyama, Toyama 930-0194, Japan. Email: nrb52665@yahoo.co.jp

Received 9 September 2013; revised 8 January 2014; accepted 23 January 2014.

Methods

We conducted a retrospective review of SCID patients with pneumothorax associated with PCP. Four patients were diagnosed with SCID on genetic analysis at the University of Toyama or Tokyo Medical and Dental University from 2003 to 2012. Informed consent was obtained from the parents of the participants. Their medical records were reviewed, and anonymous data were collected. The data included conditions related to the occurrence of pneumothorax, radiological imaging, management of respiration, use of drugs, HSCT and prognosis.

The diagnosis of PCP was made according to the presence of *Pneumocystis* DNA detected on polymerase chain reaction (PCR) assays from respiratory or gastric samples in a patient with a suspicious clinical presentation.[9]

The diagnosis of pneumothorax was made if chest X-ray or computed tomography (CT) showed a collection of air in the

Table 1 Patient characteristics, diagnosis and conditions

Patient	Age at admission (months)	Sex	Diagnosis of SCID (*IL2RG* mutation)	Lymphocyte count (3900–9000†) (/μL)	$CD3^+$ T cells (51–77†) (%)	$CD19^+$ B cells (11–41†) (%)	$CD56^+$ NK cells (3–14†) (%)	IgG level (241–613‡) (mg/dL)
1	4	Male	X-SCID (R285E)	2550	0.2	97.2	0.6	125
2	5	Male	X-SCID (C231R)	640	0.2	97.4	0.6	<100
3	5	Male	X-SCID (C102R)	2670	1.0	96.0	1.0	94
4	9	Male	X-SCID (K294X)	3000	0.0	77.1	0.5	2.7

†Reference values.[11] ‡Reference values.[12] IgG, immunoglobulin G; X-SCID, X-linked severe combined immunodeficiency.

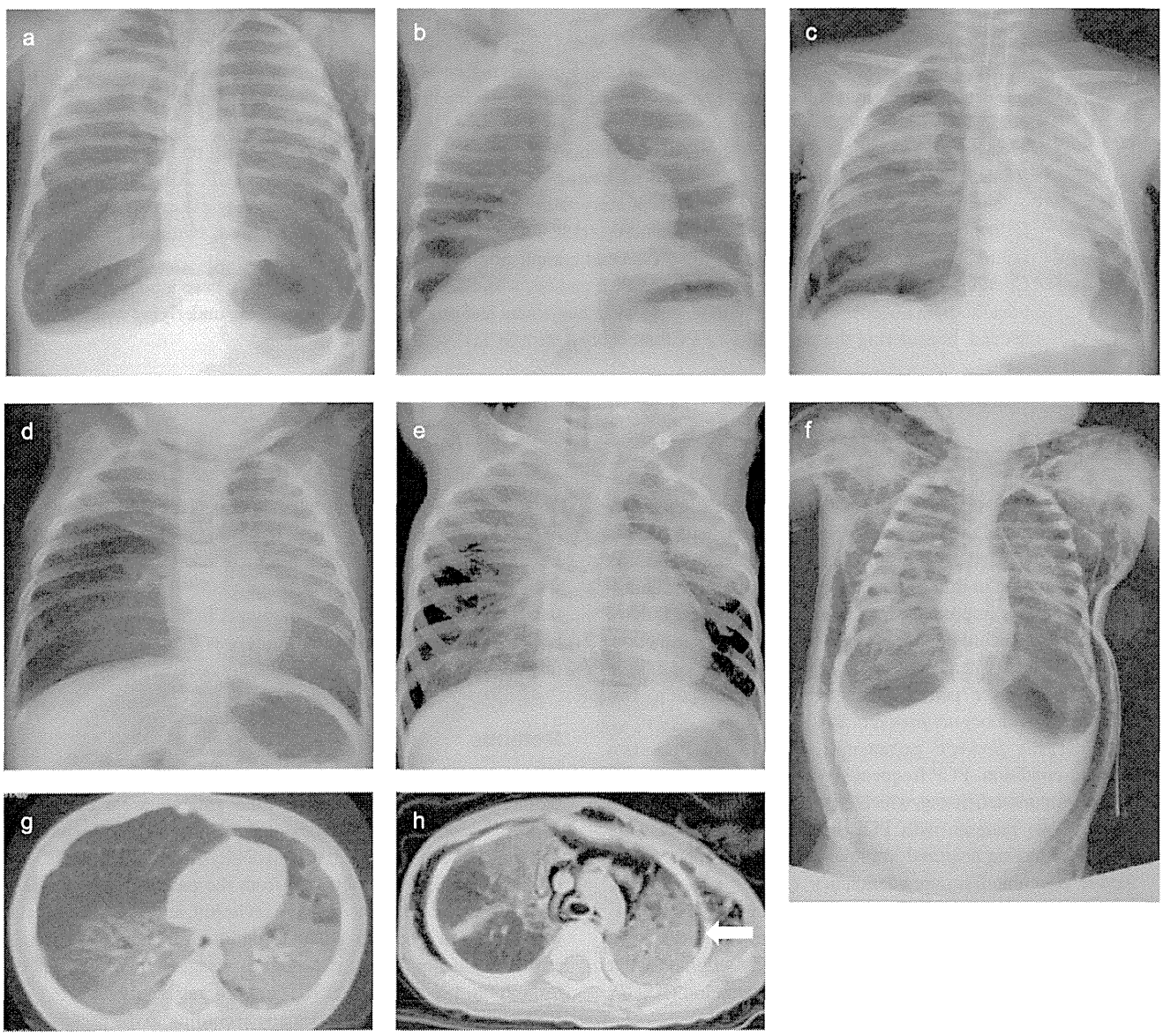

Fig. 1 Radiological imaging. (a) Bilateral pneumothorax in patient 1; (b) right pneumothorax occurring before respirator therapy in patient 2; and (c) right pneumothorax occurring during respirator therapy in patient 3. (d,g) *Pneumocystis jirovecii* pneumonia before occurrence of pneumothorax in patient 1. Focal ground-glass pattern involving the bilateral lower lobes is seen. (e,h) Pneumomediastinum and subcutaneous emphysema before occurrence of pneumothorax in patient 4. Cystic change is seen (h, arrow). (f) Subcutaneous emphysema and bilateral pneumothorax in patient 1. The thymus is not seen in all patients.

pleural space. The size of pneumothorax was classified as "small" or "large", and defined as <50% occupation of the hemithorax volume or not.[10]

Results

Patient characteristics, diagnosis and conditions are listed in Tables 1,2. All four patients had X-linked SCID caused by *interleukin 2 receptor, gamma (IL2RG)* mutations (C102R, C231R, R285E and K294X). Age at the time of SCID diagnosis ranged between 4 and 9 months at the time of contracting PCP. They had presented with respiratory symptoms only since the diagnosis of SCID. Respiratory symptoms presented before admission for 7–14 days in three patients and 90 days in one patient. PCR assay for detecting adenovirus, human metapneumovirus, parainfluenza virus, enterovirus and *Mycoplasma pneumoniae* in patient 1, and adenovirus, human metapneumovirus, cytomegalovirus, respiratory syncytial virus, bocavirus, picornavirus and *Mycobacterium tuberculosis* in patient 4 were performed, and no pathogens were detected. Three patient received live vaccines (patients 2 and 3, Bacille Calmette–Guérin [BCG]; patient 4, BCG and oral polio vaccine), but no adverse events occurred. Plasma (1-3)-β-D-glucan (β-D-glucan) level increased in two patients, and serum Krebs von den Lungen-6 (KL-6) level increased in four patients. All patients received mechanical ventilation because of severe respiratory failure. Pneumothorax occurred before respirator therapy in one patient and during respirator therapy in two patients. One patient (patient 4) had pneumomediastinum on admission, and pneumothorax occurred during respirator therapy.

Radiological imaging is shown in Figure 1. Unilateral pneumothorax was seen in three patients, and bilateral pneumothorax in one patient. The size of pneumothorax was small in all four patients. Focal ground-glass pattern was seen in all four patients, and cystic change was seen in one patient. Absence of the thymus, which is a characteristic of SCID, was detected on chest radiograph and CT in all four patients.

Treatment and prognosis are shown in Table 3. The mode of mechanical ventilation was not only intermittent mandatory ventilation or synchronized intermittent mandatory ventilation (SIMV), but also high frequency oscillation or inversed ratio ventilation (IRV) for the purpose of protecting lung. All patients received trimethoprim and sulfamethoxazole (TMP/SMX) and corticosteroids for treatment of PCP and chest tube drainage for treatment of pneumothorax. Only one patient (patient 3) was successfully extubated, and he was alive following HSCT after recovery from respiratory failure. HSCT was done in three patients, and the other two patients received HSCT before recovery from respiratory failure. Of the three patients who could not be extubated, two patients died of respiratory failure and one died of early HSCT-related complications.

Discussion

Pneumothorax associated with PCP could occur in SCID patients, although, to our knowledge, PCP-associated pneumothorax in SCID patients has not been reported. All of the current patients had not presented any symptoms before contracting PCP,

Table 2 Conditions of *Pneumocystis jirovecii* pneumonia

Patient	Symptoms before admission	Duration of symptoms before admission (days)	Occurrence of pneumothorax (days after starting respirator therapy)	Occurrence of pneumomediastinum (days after starting respirator therapy)	Detection of *Pneumocystis jirovecii* (samples)	β-DG (<20†) (U/mL)	KL-6 (<250†) (pg/mL)	P/F ratio at admission
1	Cough, wheezing	14	Bilateral, during respirator therapy (11)	During respirator therapy (11)	PCR (bronchoalveolar lavage fluids)	80.6	1150	168
2	Cough, wheezing	14	Right, on admission	On admission	PCR (transtracheal aspirated sputum)	49.9	1630	248
3	Cough, wheezing	7	Right, during respirator therapy (2)	No occurrence	PCR (transtracheal aspirated sputum)	14.4	2990	131
4	Cough	90	Left, during respirator therapy (13)	On admission	PCR (fasting gastric juice)	4.6	6393	58

†Reference values. β-DG, (1-3)-β-D-glucan; KL-6, Krebs von den Lungen-6; PCR, polymerase chain reaction; P/F ratio, PaO_2/FiO_2 ratio.

Table 3 Treatment and prognosis

Patient	Mode of mechanical ventilation	Maximum pressure (mmH_2O)	Oxygen (%)	TMP/SMX (mg/kg/day)	Other drugs (mg/kg/day)	Extubation	HSCT	Prognosis
1	APRV, HFO	18/2	40	34	mPSL 2, mPSL pulse 30	No	No	Died of respiratory failure on day 22
2	IMV, HFO	25/10	100	10	PSL 1, pentamidine 4	No	Day 17, UCBT	Died of hemophagocytic syndrome and pulmonary hemorrhage on day 35
3	SIMV, IRV	30/9	100	16	PSL 2	Day 15	Day 82, UCBT	Well 4 years after HSCT
4	IMV, HFO	17/7	100	15	mPSL 1, mPSL pulse 15	No	Day 16, UCBT	Died of respiratory failure on day 17

APRV, airway pressure release ventilation; HFO, high frequency oscillation; HSCT, hematopoietic stem cell transplantation; IMV, intermittent mandatory ventilation; IRV, inversed ratio ventilation; mPSL, methylprednisolone; PSL, prednisolone; SIMV, synchronized intermittent mandatory ventilation; TMP/SMX, trimethoprim and sulfamethoxazole; UCBT, umbilical cord blood transplantation.

and they were diagnosed as having SCID through contracting PCP. In two patients with pneumothorax or pneumomediastinum on admission, investigation of the underlying condition identified PCP and, as a result of further investigation, it became apparent that they had SCID as a further underlying condition. Therefore, when pneumothorax occurs in an infant, PCP associated with SCID should be considered as a differential diagnosis, and lymphocyte count, immunoglobulin level and thymus on radiological imaging should be carefully observed. The detection rate of β-D-glucan varies according to underlying condition.[13] The clinical usefulness of serum β-D-glucan level in SCID patients is a future issue. Serum KL-6 level was very high in patient 4, who had a long duration before diagnosis of PCP because of onset with mild symptoms. A correlation has been reported between serum KL-6 level and the duration of symptoms before diagnosis of PCP,[13] but there is no report of serum KL-6 level in PCP associated with SCID. The other two patients, who did not have pneumothorax or pneumomediastinum on admission, were diagnosed as having SCID during therapy for PCP, and pneumothorax occurred during respirator therapy. A mechanism has been proposed that includes rupture of necrotic lung tissue because of historical observations of subpleural necrosis with bleb formation and bullous changes.[14] Direct lung destruction by *P. jirovecii* or neutrophilic lung inflammation was seen to be the cause in these observations.[3,15] In addition, positive pressure ventilation is also related to lung injury.

This study suggests that SCID with PCP and pneumothorax is clinically very severe, and has a poor prognosis. All of the present patients received mechanical ventilation due to severe respiratory failure, and the majority of the patients received high pressure or a high concentration of oxygen. Patient 3, who survived, received SIMV with high positive end-expiratory pressure at first, but hypoxia continued followed by the occurrence of pneumothorax. Because changing the mode of ventilation to IRV improved the symptoms of hypoxia, the need for higher pressure was avoided. The air leak was rapidly resolved after chest tube drainage, and the chest tube was removed on day 6. The tracheal tube was removed on day 15, and the patient received TMP/SMX for 30 days. When respiration is managed with mechanical ventilation in a patient with PCP, protection of the lungs should be especially considered.

The reason why SCID patients with pneumothorax have poor prognosis is not clear, but SCID patients cannot survive without successful HSCT. Non-SCID infants with pneumothorax have a good prognosis although they have severe respiratory failure.[16,17] It can be expected that approximately 90% of SCID patients will achieve long-term survival if they undergo HSCT from an HLA-matched related donor.[5] The survival rate is inferior, however, in SCID patients with poor general condition or infection at the time of HSCT.[5] Of the present three patients who received HSCT, two received HSCT before recovery from respiratory failure. There is a possibility that hypercytokinemia or pulmonary edema induced by HSCT was related to the exacerbation of HSCT-related complications or respiratory failure.[18,19] Indeed, these two patients died of early HSCT-related complications or respiratory failure.

There is no universally accepted treatment for PCP and pneumothorax associated with SCID, but the present results suggest that treatment should include TMP/SMX and corticosteroids, protection of the lungs during respirator therapy, and HSCT after recovery from respiratory failure.

This study was a retrospective analysis of data in SCID patients. There may be additional patients who were not diagnosed with SCID but who died before appropriate diagnosis and treatment. This study cannot state whether the prognosis is poor because of complications associated with pneumothorax or because pneumothorax occurs due to severe PCP.

If pneumothorax occurs in infants, both respiratory management and prompt investigation of the underlying conditions are needed, considering the possibility of PCP associated with SCID. Furthermore, pre-symptomatic diagnosis of SCID would prevent mortality in such patients. Population-based newborn screening for SCID using T-cell receptor excision circles assay is now being carried out in several countries, and the screening method can identify newborns with SCID before they contract infection.[20] We hope that this screening will become widespread.

Acknowledgments

We would like to thank the patients and families for their cooperation in this study.

References

1 Johnson NN, Toledo A, Endom EE. Pneumothorax, pneumomediastinum, and pulmonary embolism. *Pediatr. Clin. North Am.* 2010; **57**: 1357–83.
2 Alter SJ. Spontaneous pneumothorax in infants: A 10-year review. *Pediatr. Emerg. Care* 1997; **13**: 401–3.
3 Thomas CF Jr, Limper AH. Pneumocystis pneumonia. *N. Engl. J. Med.* 2004; **350**: 2487–98.
4 van der Burg M, Gennery AR. Educational paper. The expanding clinical and immunological spectrum of severe combined immunodeficiency. *Eur. J. Pediatr.* 2011; **170**: 561–71.
5 Gennery AR, Slatter MA, Grandin L *et al.* Transplantation of hematopoietic stem cells and long-term survival for primary immunodeficiencies in Europe: Entering a new century, do we do better? *J. Allergy Clin. Immunol.* 2010; **126**: 602–10.
6 Yee A, De Ravin SS, Elliott E, Ziegler JB. Severe combined immunodeficiency: A national surveillance study. *Pediatr. Allergy Immunol.* 2008; **19**: 298–302.
7 Berrington JE, Flood TJ, Abinun M, Galloway A, Cant AJ. Unsuspected Pneumocystis carinii pneumonia at presentation of severe primary immunodeficiency. *Arch. Dis. Child.* 2000; **82**: 144–7.
8 Deerojanawong J, Chang AB, Eng PA, Robertson CF, Kemp AS. Pulmonary diseases in children with severe combined immune deficiency and DiGeorge syndrome. *Pediatr. Pulmonol.* 1997; **24**: 324–30.
9 Wakefield AE, Pixley FJ, Banerji S *et al.* Detection of Pneumocystis carinii with DNA amplification. *Lancet* 1990; **336**: 451–3.
10 MacDuff A, Arnold A, Harvey J. Management of spontaneous pneumothorax: British Thoracic Society Pleural Disease Guideline 2010. *Thorax* 2010; **65** (Suppl. 2): ii18–31.
11 Shearer WT, Rosenblatt HM, Gelman RS *et al.* Lymphocyte subsets in healthy children from birth through 18 years of age: The Pediatric AIDS Clinical Trials Group P1009 study. *J. Allergy Clin. Immunol.* 2003; **112**: 973–80.
12 Stiehm ER, Fudenberg HH. Serum levels of immune globulins in health and disease: A survey. *Pediatrics* 1966; **37**: 715–27.
13 Nakamura H, Tateyama M, Tasato D *et al.* Clinical utility of serum beta-D-glucan and KL-6 levels in Pneumocystis jirovecii pneumonia. *Intern. Med.* 2009; **48**: 195–202.
14 Beers MF, Sohn M, Swartz M. Recurrent pneumothorax in AIDS patients with Pneumocystis pneumonia. A clinicopathologic report of three cases and review of the literature. *Chest* 1990; **98**: 266–70.
15 Eng RH, Bishburg E, Smith SM. Evidence for destruction of lung tissues during Pneumocystis carinii infection. *Arch. Intern. Med.* 1987; **147**: 746–9.
16 Ursic T, Steyer A, Kopriva S, Kalan G, Krivec U, Petrovec M. Human bocavirus as the cause of a life-threatening infection. *J. Clin. Microbiol.* 2011; **49**: 1179–81.
17 Piastra M, Onesimo R, De Luca D *et al.* Measles-induced respiratory distress, air-leak and ARDS. *Eur. J. Clin. Microbiol. Infect. Dis.* 2010; **29**: 181–5.
18 Takagi S, Masuoka K, Uchida N *et al.* High incidence of haemophagocytic syndrome following umbilical cord blood transplantation for adults. *Br. J. Haematol.* 2009; **147**: 543–53.
19 Michelson PH, Goyal R, Kurland G. Pulmonary complications of haematopoietic cell transplantation in children. *Paediatr. Respir. Rev.* 2007; **8**: 46–61.
20 Buckley RH. The long quest for neonatal screening for severe combined immunodeficiency. *J. Allergy Clin. Immunol.* 2012; **129**: 597–604.

Journal of the Neurological Sciences 340 (2014) 86–90

Contents lists available at ScienceDirect

Journal of the Neurological Sciences

journal homepage: www.elsevier.com/locate/jns

Whole-exome sequence analysis of ataxia telangiectasia-like phenotype

Setsuko Hasegawa [a], Kohsuke Imai [a], Kenichi Yoshida [b,e], Yusuke Okuno [b], Hideki Muramatsu [c], Yuichi Shiraishi [f], Kenichi Chiba [f], Hiroko Tanaka [d], Satoru Miyano [d], Seiji Kojima [c], Seishi Ogawa [b,e], Tomohiro Morio [a], Shuki Mizutani [a], Masatoshi Takagi [a,*]

[a] Department of Pediatrics and Developmental Biology, Tokyo Medical and Dental University, Tokyo, Japan
[b] Cancer Genomics Project, Graduate School of Medicine, University of Tokyo, Tokyo, Japan
[c] Department of Pediatrics, Nagoya University Graduate School of Medicine, Nagoya, Japan
[d] Laboratory of Sequence Analysis, Human Genome Center, Institute of Medical Science, The University of Tokyo, Tokyo, Japan
[e] Department of Pathology and Tumor Biology, Graduate School of Medicine, Kyoto University, Kyoto, Japan
[f] Laboratory of DNA Information Analysis, Human Genome Center, Institute of Medical Science, The University of Tokyo, Tokyo, Japan

ARTICLE INFO

Article history:
Received 2 December 2013
Received in revised form 21 February 2014
Accepted 25 February 2014
Available online 4 March 2014

Keywords:
Whole-exome sequencing
Neurodegeneration
Immunodeficiency
CD40 ligand
SIL1
DNA damage

ABSTRACT

A number of diseases exhibit neurodegeneration with/without additional symptoms such as immunodeficiency, increased cancer risk, and microcephalus. Ataxia telangiectasia and Nijmegen breakage syndrome, for example, develop as a result of mutations in genes involved in the DNA damage response. However, such diseases can be difficult to diagnose as they are only rarely encountered by physicians. To overcome this challenge, nine patients with symptoms that resemble those of ataxia telangiectasia, including neurodegeneration, hypogammaglobulinemia, telangiectasia, and/or elevated serum α-fetoprotein, were subjected to whole-exome sequencing (WES) to identify the causative mutations. Molecular diagnosis was achieved in two patients: one displayed CD40 ligand (CD40LG) deficiency, while a second showed a homozygous *SIL1* mutation, which has been linked to Marinesco-Sjögren syndrome (MSS). Typical features of CD40LG deficiency and MSS are distinct from the symptoms usually seen in ataxia telangiectasia. These dissociations between phenotype and genotype make it difficult to achieve molecular diagnosis of orphan diseases. Whole-exome sequencing analyses will assist in the molecular diagnosis of such cases and allow the identification of genotypes that would not be expected from the phenotype.

1. Introduction

Neurodegenerative disease is characterized by progressive nervous system dysfunction. Primary immunodeficiency is a disorder of immune regulation. Occasionally, progressive nervous system dysfunction and primary immunodeficiency can occur together within single disorders, and the genes responsible for such conditions have been identified. Ataxia telangiectasia (A-T) is one such disorder involving progressive cerebellar ataxia and immunodeficiency, as well as conjunctival telangiectasia. The gene responsible, *ATM*, plays a central role in the DNA damage response (DDR) [1]. Mutations of *NBS1* and *Mre11*, genes also involved in DDR network, can give rise to phenotypically A-T-like patients, such as those with Nijmegen breakage syndrome (NBS) and A-T-like disease (ATLD). Not only NBS and ATLD, but also a number of diseases also feature both neurological symptoms and immunodeficiency. Gatti et al. proposed a disease category named XCIND (X-ray irradiation sensitivity, Cancer susceptibility, Immunodeficiency, Neurological abnormality, Double strand DNA breakage) syndrome [2], in which failure of the DDR pathway results in genome instability and an increased risk of cancer. A number of human genetic disorders are characterized by a defective DDR pathway and feature neurodegeneration, which suggests that maintaining genome stability is also important for preserving post-mitotic neurons [3].

Pediatric neurodevelopmental disorders comprise various diseases with multi-system symptoms. Some of the features characteristic of these diseases appear only in later years, and some patients only manifest non-specific symptoms, leading to a delayed diagnosis. In certain cases, different phenotypes can arise from the same genotype. For example, mutation of SETX, which is involved in DDR, can give rise to three distinct types of disease: ataxia-ocular apraxia-2 (AOA2), autosomal recessive spinocerebellar ataxia (SCA) 1, and juvenile amyotrophic lateral sclerosis (ALS) 4. In the present study, nine patients with clinical features of neurodegeneration, hypogammaglobulinemia and/or telangiectasia were analyzed by whole-exome sequencing (WES). The

* Corresponding author at: Department of Pediatrics and Developmental Biology, Graduate Medical School, Tokyo Medical and Dental University, Yushima 1-5-45, Bunkyo-ku, Tokyo 113-8519, Japan. Tel.: +81 3 5803 5249; fax: +81 3 5803 5247.
E-mail address: m.takagi.ped@tmd.ac.jp (M. Takagi).

http://dx.doi.org/10.1016/j.jns.2014.02.033
0022-510X/

results reveal that one patient had CD40LG deficiency and that another patient had Marinesco–Sjögren syndrome (MSS).

2. Materials and methods

2.1. Patient samples

Patients with neurological symptoms resembling an A-T-like phenotype, comprised mainly of cerebellar ataxia plus hypogammaglobulinemia, telangiectasia and/or elevated serum alpha-fetoprotein (AFP), were recruited. ATM western blotting was performed with these patients to exclude A-T. Patients with normal ATM levels were subjected to WES.

Patients provided informed written consent, and the experimental design was approved by the ethics committee at Tokyo Medical and Dental University (No. 103).

2.2. Whole-exome sequencing analysis (WES)

WES analysis was performed as previously described [4]. Briefly, genomic DNA was fragmented, and exonic sequences were enriched using SureSelect Target Enrichment with the SureSelect Human All Exon 38 Mb kit (Agilent). The captured fragments were purified and sequenced on an Illumina Hiseq2000 platform using paired-end reads. Bioinformatic analysis was performed using an in-house algorithm based on published tools. Identified single nucleotide variants (SNVs) were filtered using dbSNP version 131 and 132, the 1000 Genomes database, an in-house SNP database, and the Human Genetic Variation Database (HGVD) (http://www.genome.med.kyoto-u.ac.jp/SnpDB/).

2.3. Genome sequencing

The mutations identified by WES were confirmed by direct sequencing. Genomic DNA from peripheral blood mononuclear cells was obtained using the QIAamp DNA Mini kit (Qiagen). Exons of the respective genes were amplified by PCR. Nucleotide sequencing was performed by cycle sequencing using ABI BigDye Terminator chemistry (Applied Biosystems) followed by capillary electrophoresis on an ABI 3100 automated sequencer.

2.4. CD40LG expression analysis

CD40LG expression was measured by flow cytometry using activated T-cells [5]. Cells were treated with phosphate-buffered saline (PBS) or PMA/ionomycin, and incubated for 4 h. CD40LG expression in T-cell gates was monitored by phycoerythrin (PE)-conjugated anti-human CD40LG antibody (Beckman Coulter), combined with the T-cell marker CD3 (PC 5-conjugated anti-CD3 antibody: Beckman Coulter). Flow cytometric analysis was performed using FACS Caliber with the CellQuest program (Becton-Dickinson).

2.5. Western blotting

Cells were lysed in RIPA buffer (50 mM Tris–HCl (pH 7.5), 150 mM NaCl, 0.5% sodium deoxycholate, 0.1% SDS, phosphatase, and a protease inhibitor cocktail). Samples were resolved on SDS-polyacrylamide gels. The gels were transferred to nitrocellulose membranes (Millipore) and blocked with 5% nonfat milk. The membranes were incubated with the appropriate anti-SIL1 (Abcam), anti-β-actin (Sigma), anti-eIF2α, and anti-phospho-eIF2α (Cell Signaling) antibodies. Primary antibodies were detected by binding horseradish peroxidase (HRP)-conjugated anti-rabbit or anti-mouse secondary antibody with an ECL kit (GE Healthcare).

3. Results

Patients presenting with more than two features of ataxia or other neurological degeneration symptoms and hypogammaglobulinemia, telangiectasia and/or elevated serum AFP were examined in this study (Table 1). Most of the causative ATM mutations in typical A-T patients are truncating, and ATM protein is therefore absent in these patients [6]. Western blot analysis confirmed ATM protein expression in all of the subjects in this study (data not shown). Furthermore, WES analysis failed to identify an ATM mutation, and thus A-T was ruled out in these subjects. We speculated that these patients had XCIND syndrome. WES revealed 238 non-synonymous SNV, frameshift, or splice site mutations. Although SNVs located within DDR-related genes were identified (Supplementary Table 1), no mutations were seen in the genes responsible for XCIND (data not shown). Intriguingly, a hemizygous *CD40LG* mutation and a homozygous *SIL1* mutation were identified in patients 1 and 5, respectively.

3.1. Patient 1

Patient 1 is a 21-year-old male and a child of non-consanguineous healthy Japanese parents. He has no familial history of any immunological disorders, while his grandfather suffered from Parkinson's disease. He showed normal motor development during infancy, but failed to thrive. Due to recurrent otitis media, he was presumed to have a primary immune deficiency of unknown origin, and began intravenous immunoglobulin treatment every 2 weeks at 12 months of age. In childhood, he manifested clumsiness, and an asymmetrical arm motion was identified during walking at 16 years of age. At 20 years, he developed involuntary movements that were induced by eating and that deteriorated over a few days. He was admitted with involuntary movements of the extremities; he was alert and conscious. His intelligence quotient was 58. He had mild dysarthria. Neurologic examinations

Table 1
Clinical features of patients.

patient	Sex	Age (years)	Immunodeficiency	Neurological symptoms	Telangiectasia	Serum AFP
1	M	21	Recurrent otitis media, low IgG, and elevated IgM	Choreoathetosis, dysarthria, hyperreflexia, psychomotor retardation, and cerebral cortex atrophy	−	NE
2	F	5	-	Ataxia and cerebellar atrophy	+	Normal
3	F	21	Low IgA and normal IgG and IgM	Nystagmus, dysarthria, hypotonus, myoclonus, ataxia, hyporeflexia, and cerebellar atrophy	+	Normal
4	F	2	Low IgG	Psychomotor retardation and regression	−	Elevated
5	M	1	Low IgG and IgG_2 subclass and normal IgM	Gross motor developmental delay, nystagmus, and cerebellar atrophy	−	Normal
6	F	1	-	Myoclonus, choreoathetosis, psychomotor retardation, and epilepsy	−	Elevated
7	F	11	Aspergillosis and low IgA, IgG and IgM	Psychomotor retardation and epilepsy	−	Normal
8	F	7	Oral candidiasis, *Pneumocystis carinii* pneumonia, and low IgA, IgG and IgM	Psychomotor retardation	−	NE
9	F	5	Low IgM and reduced B cell number	Ataxia, mental retardation, and microcephaly	+	NE

NE: not examined.

showed involuntary movements of the limbs, face, and trunk. This non-rhythmic involuntary movement appeared dominant in the right arm, and was induced by motor action. This movement did not occur during sleep. The deep tendon reflex was markedly hyperactive in the bilateral ankle clonus, but there was no pathological reflex.

Laboratory data showed normal complete blood cell count with no acanthocytes. Electrolyte and hepato-renal functions were within normal limits, and euthyroidism was confirmed. Serological examination showed low serum levels of IgG (687 mg/dl) and elevated serum IgM (462 mg/dl). Serum ceruloplasmin levels were normal, and the autoantibodies, anti-streptolysin O and anti-streptokinase antibodies, were negative. The cerebrospinal fluid cell count was 21 cells/mm^3 and comprised 100% mononuclear cells. Protein and glucose concentrations were 21 mg/dl and 54 mg/dl, respectively. No pathogens indicating infection were identified. There was no calcification at the time of brain computed tomography (CT). Brain magnetic resonance imaging (MRI) revealed cerebral cortex atrophy without abnormal signal intensity and atrophy of the striatum (Fig. 1). Electroencephalography demonstrated generalized intermittent slow waves and focal sharp waves over the bilateral occipital region. He had no clinical seizures. Within 6 months, he was unable to walk or sit unaided, as a consequence of choreoathetosis.

WES identified a *CD40LG* mutation in this patient, which was validated by Sanger sequencing (Fig. 2A). A functional assay for CD40LG expression confirmed that the mutation impaired CD40LG functioning (Fig. 2B).

3.2. Patient 5

Patient 5 is a 14-month-old male and a child of non-consanguineous healthy Japanese parents. He has no familial history of any immunological disorder. His sister (6 years old) and brother (3 years old) have had several febrile seizures. He was born uneventfully, and showed mild developmental delay. He was able to hold his head up at 10 months of age, rolled over at 12 months, and has yet to sit up and crawl. He showed nystagmus at 12 months and his brain MRI revealed cerebellar atrophy (Fig. 3). Serological examination showed relatively low serum levels of IgG (490 mg/dl), IgG$_2$ subclass (18%), and IgA (15 mg/dl) and normal serum levels of IgM (68 mg/dl). Opportunistic infections or recurrent

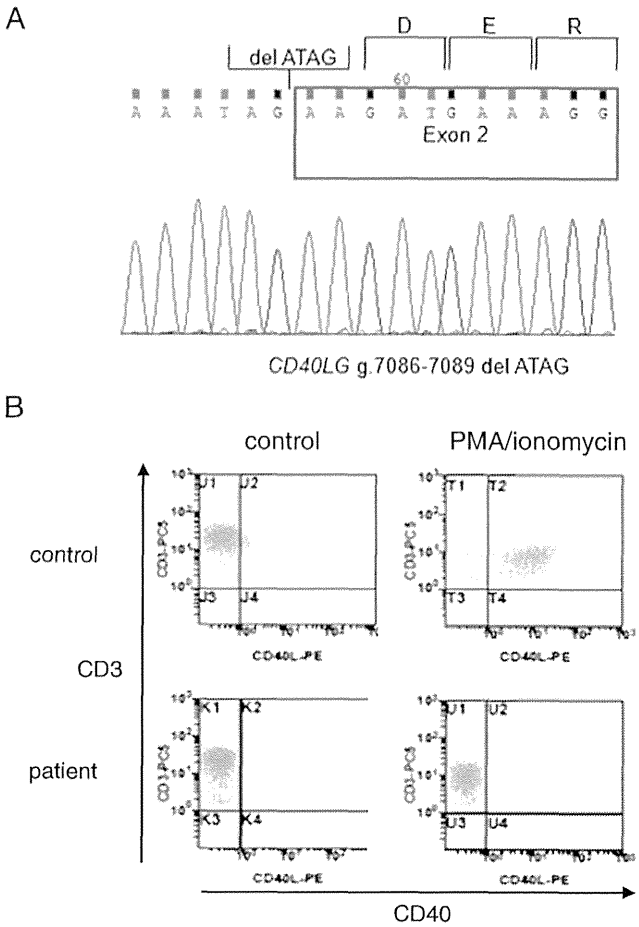

Fig. 2. A, Sequence electropherogram of *CD40LG*. A hemizygous frameshift mutation was identified. B, PMA/ionomycin treatment induced CD40LG expression. 88.68% of CD3$^+$CD8$^-$ cells were positive for CD40LG in healthy controls. On the other hand, only 0.82% were positive in patient-derived activated T-cells.

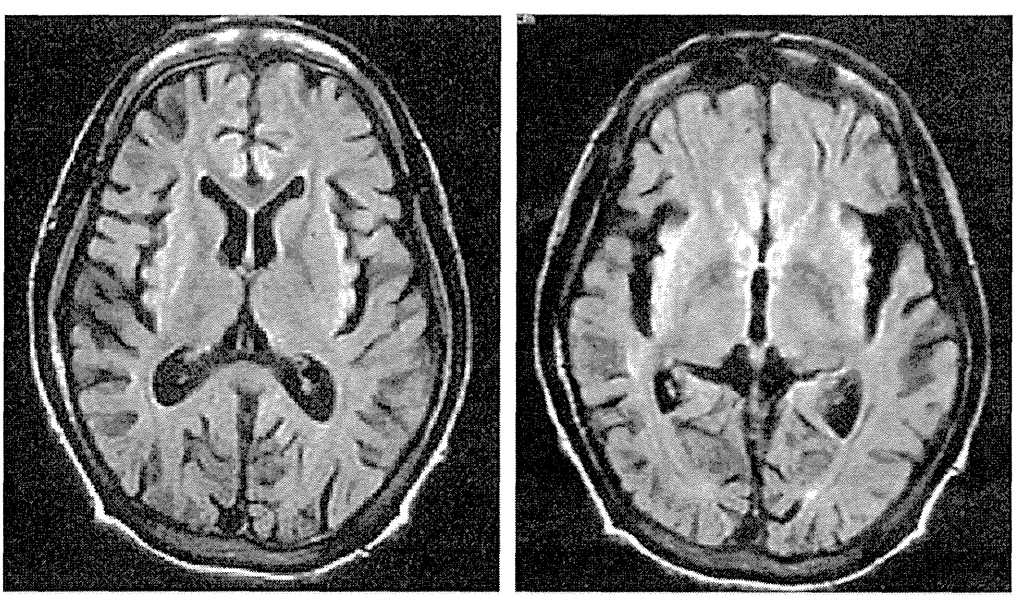

Fig. 1. Fluid attenuated inversion recovery axial images of patient 1, demonstrating cerebral cortical atrophy.

infections have not been observed in this patient. Cerebrospinal fluid analysis was normal, as were levels of pyruvate and lactate.

Although hypoglobulinemia has not been previously reported in MSS, WES identified a homozygous frameshift mutation in *SIL1*, c.936_937ins G, which was validated by Sanger sequencing (Fig. 4A). SIL1 expression was markedly decreased in a patient-derived EB virus-transformed lymphoblastoid cell line (Fig. 4B). SIL1 functions in combination with binding immunoglobulin protein (BiP) to ensure proper folding of proteins in the endoplasmic reticulum (ER) [7]. Accumulation of misfolded proteins suppresses de novo protein synthesis via translation inhibition. eIF2α is involved in this process. ER stress induces phosphorylation of eIF2α on serine 51 [8]. The patient-derived EB virus-transformed lymphoblastoid cell line exhibited increased phosphorylation of eIF2α, suggesting increased ER stress (Fig. 4C).

4. Discussion

A splice acceptor mutation of *CD40LG* was identified in patient 1, and CD40LG expression was lower in this patient (Fig. 2B). This *CD40LG* mutation has previously been reported in hyper IgM syndrome (HIGM) [9], but neurodegeneration is not a common feature of HIGM disorder. We speculated that mutations in other genes were probably the cause of the atypical symptoms seen in our patient. A heterozygous non-frameshift deletion (c.1242_1244 del) in *POLG* (DNA polymerase subunit γ gene), which has not been described before, was identified as a candidate. *POLG* is essential for mitochondrial DNA (mtDNA) replication. Mutations in *POLG* have been identified in various diseases such as progressive external ophthalmoplegia (PEO), Alpers syndrome and other infantile hepatocerebral syndromes, ataxia-neuropathy syndromes, Charcot–Marie–Tooth disease, and idiopathic parkinsonism [10]. These diseases are characterized by mtDNA depletion in symptomatic tissues. Although a *POLG* in-frame nucleotide deletion was identified in patient 1, mtDNA levels were the same as in the other patients, suggesting that this in-frame nucleotide deletion does not interfere with POLG function (data not shown). This result suggests that the neurological symptoms in this patient are very unlikely to be modified by mutation of *POLG*.

Patients with CD40LG deficiency are susceptible to central nervous system (CNS) infections. The incidence of CNS infection or progressive neurodegeneration is 12–16% among patients with CD40LG deficiency [11]. Dysfunction of CD40–CD40LG dependent T-cell immunity attenuates $CD8^+$ T-cell trafficking to the CNS in mice, and this led to elevated West Nile virus titers and resulted in neurodegeneration [12]. Immunodeficiency caused by CD40LG deficiency can increase susceptibility to CNS infection, or allow persistent CNS infection, and this can explain the neurodegeneration observed in patients. Bishu et al. reported five patients exhibiting neurological symptoms, including ataxia, in a cohort of 31 patients. Although an infectious etiology is the most plausible explanation, no pathogens were identified in four of the patients with neurological symptoms. This group proposed that the lack of proof of infection necessitates consideration of other etiologies [13], which may also be the case with our patient. There are several interesting previous reports suggesting a relationship between CD40–CD40LG function and neuronal function. CD40LG is critical for protection from demyelinating disease and for development of spontaneous remyelination in a mouse model of multiple sclerosis produced by infection with Theiler's murine encephalomyelitis virus [14]. CD40–CD40LG interaction enables astrocytosis and microgliosis in response to amyloid-beta peptide [15]. Although CD40LG deficiency does not lead directly to neurodegeneration, CD40 is expressed and functional on mouse and human neurons. CD40-deficient mice display neuronal dysfunction, aberrant neuronal morphology, and associated gross brain abnormalities [16]. These findings suggest that an infection-based hypothesis is not the only possibility; changes in neuronal function could also explain the neurodegeneration seen as a result of CD40LG deficiency.

Mutation in *SIL1* causes MSS [17], an autosomal recessive disorder that is principally associated with cerebellar ataxia, bilateral cataracts, myopathy and mental retardation. The mutation seen in patient 5 in

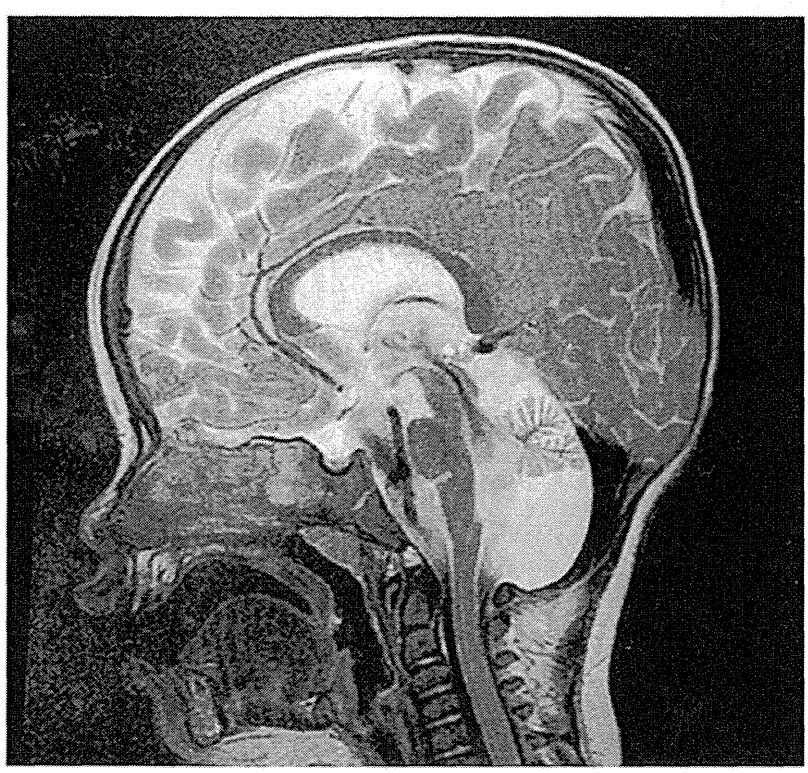

Fig. 3. Sagittal midline T2-weighted MR image of patient 5, demonstrating cerebellar atrophy of the vermis.

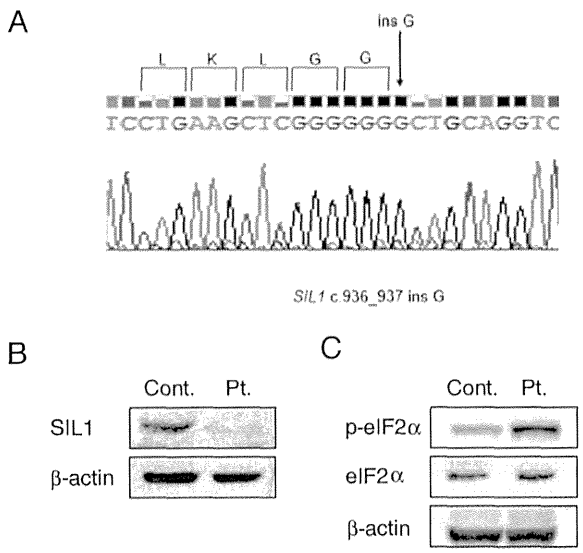

Fig. 4. A, Sequence electropherogram of *SIL1*. A homozygous frameshift mutation was identified. B, Western blotting analysis of SIL1 expression. C, eIF2α and phosphorylated eIF2α (p-eIF2α) levels. Cont: protein extract from EBV-transformed lymphoblastoid cell line derived from a healthy volunteer. Pt: protein extract from EBV-transformed lymphoblastoid cell line derived from patient 5.

this study was also reported in three unrelated Japanese patients with MSS [18]. Patient 5 did not demonstrate cataracts at 1 year of age, although cataracts are known to appear later in life [17]. Although hypogammaglobulinemia has not been previously described in MSS, patient 5 exhibited remarkably reduced levels of serum IgG_2 with a moderate decrease in total IgG and IgA levels. SIL1 functions in combination with BiP to ensure proper folding of proteins in the ER [7]. Assembly of the immunoglobulin heavy chain and light chain is performed in the ER in association with the ER chaperone, BiP [19]. In this study, we have not examined if hypogammaglobulinemia is a common feature of MSS or a specific feature of this case 5 patient. A further study of cases is therefore needed to reveal whether hypogammaglobulinemia is a common feature in MSS.

Several non-synonymous SNV, frameshift, or splice site mutations in DDR-associated genes were identified (Supplementary Table 1). Further studies are required to evaluate the functional effects of these SNVs.

Molecular genotypes are occasionally obscured by exogenous or endogenous factors, infections, treatments or the disease process. In addition, these factors can sometimes hinder the identification of causative mutations. Recent advances in genome analysis technology allow the identification of such mutations in subjects with indistinguishable phenotypes, and this can lead to an unpredictable molecular diagnosis for these patients. However, many of the well-known hereditary ataxias, including SCA, dentatorubral-pallidoluysian atrophy (DRPLA), and Friedreich's ataxia, are caused by tri-nucleotide expansions. In these cases, WES analysis may fail to identify the causative mutation. In fact, molecular diagnoses for the other seven patients in the present study remain elusive. A combination of copy number and WES analyses of family members may increase the sensitivity and accuracy of genetic diagnosis. WES analyses will help to diagnose cases in which symptoms have been altered by infections or concomitant multiple gene alterations.

Conflicts of interest

The authors declare that they have no conflicts of interest.

Acknowledgments

The authors would like to thank the patients and their families for sharing this information. This work was supported by Grants-in-Aid 'the Research on Measures for Intractable Diseases Project' from the Ministry of Health, Labor and Welfare of Japan (H23-012).

Appendix A. Supplementary data

Supplementary data to this article can be found online at http://dx.doi.org/10.1016/j.jns.2014.02.033.

References

[1] Shiloh Y. ATM and related protein kinases: safeguarding genome integrity. Nat Rev Cancer 2003;3(3):155–68.
[2] Gatti RA, Boder E, Good RA. Immunodeficiency, radiosensitivity, and the XCIND syndrome. Immunol Res 2007;38(1–3):87–101.
[3] Lavin MF, Gueven N, Grattan-Smith P. Defective responses to DNA single- and double-strand breaks in spinocerebellar ataxia. DNA Repair 2008;7(7):1061–76.
[4] Kunishima S, Okuno Y, Yoshida K, Shiraishi Y, Sanada M, Muramatsu H, et al. *ACTN1* mutations cause congenital macrothrombocytopenia. Am J Hum Genet 2013;92(3):431–8.
[5] Tomizawa D, Aoki Y, Nagasawa M, Morio T, Kajiwara M, Sekine T, et al. Novel adopted immunotherapy for mixed chimerism after unrelated cord blood transplantation in Omenn syndrome. Eur J Haematol 2005;75(5):441–4.
[6] Buzin CH, Gatti RA, Nguyen VQ, Wen CY, Mitui M, Sanal O, et al. Comprehensive scanning of the ATM gene with DOVAM-S. Hum Mutat 2003;21(2):123–31.
[7] Van Raamsdonk JM. Loss of function mutations in SIL1 cause Marinesco–Sjogren syndrome. Clin Genet 2006;69(5):399–400.
[8] Donnelly N, Gorman AM, Gupta S, Samali A. The eIF2alpha kinases: their structures and functions. Cell Mol Life Sci 2013;70(19):3493–511.
[9] Lee WI, Torgerson TR, Schumacher MJ, Yel L, Zhu Q, Ochs HD. Molecular analysis of a large cohort of patients with the hyper immunoglobulin M (IgM) syndrome. Blood 2005;105(5):1881–90.
[10] Chan SS, Copeland WC. DNA polymerase gamma and mitochondrial disease: understanding the consequence of *POLG* mutations. Biochim Biophys Acta 2009;1787(5):312–9.
[11] Levy J, Espanol-Boren T, Thomas C, Fischer A, Tovo P, Bordigoni P, et al. Clinical spectrum of X-linked hyper-IgM syndrome. J Pediatr 1997;131(1 Pt 1):47–54.
[12] Sitati E, McCandless EE, Klein RS, Diamond MS. CD40–CD40 ligand interactions promote trafficking of CD8+ T cells into the brain and protection against West Nile virus encephalitis. J Virol 2007;81(18):9801–11.
[13] Bishu S, Madhavan D, Perez P, Civitello L, Liu S, Fessler M, et al. CD40 ligand deficiency: neurologic sequelae with radiographic correlation. Pediatr Neurol 2009;41(6):419–27.
[14] Drescher KM, Zoecklein LJ, Pavelko KD, Rivera-Quinones C, Hollenbaugh D, Rodriguez M. CD40L is critical for protection from demyelinating disease and development of spontaneous remyelination in a mouse model of multiple sclerosis. Brain Pathol 2000;10(1):1–15.
[15] Tan J, Town T, Crawford F, Mori T, DelleDonne A, Crescentini R, et al. Role of CD40 ligand in amyloidosis in transgenic Alzheimer's mice. Nat Neurosci 2002;5(12):1288–93.
[16] Hou H, Obregon D, Lou D, Ehrhart J, Fernandez F, Silver A, et al. Modulation of neuronal differentiation by CD40 isoforms. Biochem Biophys Res Commun 2008;369(2):641–7.
[17] Anttonen AK, Mahjneh I, Hamalainen RH, Lagier-Tourenne C, Kopra O, Waris L, et al. The gene disrupted in Marinesco–Sjogren syndrome encodes SIL1, an HSPA5 cochaperone. Nat Genet 2005;37(12):1309–11.
[18] Eriguchi M, Mizuta H, Kurohara K, Fujitake J, Kuroda Y. Identification of a new homozygous frameshift insertion mutation in the SIL1 gene in 3 Japanese patients with Marinesco–Sjogren syndrome. J Neurol Sci 2008;270(1–2):197–200.
[19] Lee YK, Brewer JW, Hellman R, Hendershot LM. BiP and immunoglobulin light chain cooperate to control the folding of heavy chain and ensure the fidelity of immunoglobulin assembly. Mol Biol Cell 1999;10(7):2209–19.